

CLARIFYING THE EFFECT OF MEAN SUBTRACTION ON DYNAMIC MODE DECOMPOSITION

GOWTHAM S SEENIVASAHARAGAVAN*, MILAN KORDA†, HASSAN ARBABI ‡, AND IGOR MEZIĆ§

Abstract. Any autonomous nonlinear dynamical system can be viewed as a superposition of infinitely many linear processes, through the so-called Koopman mode decomposition. Its data-driven approximation- Dynamic Mode Decomposition (DMD)- has been extensively developed and deployed across a plethora of fields. In this work, we study the effect of subtracting the temporal mean on the DMD approximation, for observables possessing only a finite number of Koopman modes.

Pre-processing time-sequential training data by removing the temporal mean has been a point of contention in the Companion matrix formulation of DMD. This stems from the potential of said pre-processing to render DMD equivalent to a temporal Discrete Fourier Transform (DFT). We prove that this equivalence is impossible when the training data is linearly consistent and the order of the DMD approximation exceeds the number of Koopman modes. Since model order and training set size are synonymous in this variant of DMD, the parity of DMD and DFT can, therefore, be indicative of inadequate training data.

Key words. Koopman operator, Dynamic Mode Decomposition, Companion matrix, Mean subtraction, Discrete Fourier Transform.

AMS subject classifications. 37M10, 37N10, 47N20

1. Introduction. Models of nonlinear phenomena are particularly useful when they strike a balance between simplicity and generalizability. Such balanced models can be constructed in a principled and rigorous fashion through the Koopman operator [11, 16, 14]. This object is typically infinite-dimensional, but is always linear. Hence, the eigenfunctions of the Koopman operator can be used to build generalizable linear models of non-linear dynamics. Consequently, algorithms for computing these spectral quantities have been the focus of sustained research. A substantial fraction of these efforts concerns the so-called Dynamic Mode Decomposition (DMD) [20, 22, 25].

Procedurally, DMD is simply a linear fit followed by an eigen-decomposition. Hence, it has been applied to data from a plethora of natural and engineered phenomena; see for example the survey [6]. In parallel, theoretical investigations have probed the effect of time delays, choice of observables and convergence to Koopman spectral quantities- see [12] as well as the reviews [23] and [17] for a detailed discussion. This work continues the conversation on the pragmatic issue of removing the temporal mean, and its theoretical implications for DMD.

The infinite-time average, when it exists, is the leading term of the Koopman mode decomposition [14]. Its removal brings focus on the temporally varying parts of the process, and has been adopted in a diverse set of analyses [4, 19, 21, 3]. Nonetheless, in practice, this step may render DMD equivalent to a temporal Discrete Fourier Transform (DFT) [7]. The negative consequences of such an equivalence include the misrepresentation of dissipative dynamics and a bijection between the trajectory length and the DMD-based estimates of the Koopman eigenvalues.

The relationship between mean-subtracted DMD and DFT is substantially clarified in a subsequent work by Hirsch and co-workers [9]. Although their primary

*Department of Mechanical Engineering, University of California Santa Barbara

†Methods and Algorithms for Control, LAAS-CNRS

‡Department of Mechanical Engineering, Massachusetts Institute of Technology

§Department of Mechanical Engineering, University of California Santa Barbara

contribution is an *alternative* to temporal mean removal, they also study the original pre-processing step in itself. First, they point out that the original work [7] only provides a *sufficient* condition for the equivalence of mean-subtracted DMD and DFT. Then, assuming the observables used in DMD possess only a finite number of Koopman modes, they prove that the sufficiency condition is not satisfied when certain sub-matrices of the training set are connected by a linear map (linear consistency) and the training set size exceeds the number of Koopman modes (over-sampling). Finally, they provide numerical evidence that suggests linear consistency and over-sampling can actually negate DMD-DFT equivalence, i.e., be a sufficient condition for non-equivalence.

We begin by developing a *necessary and sufficient condition* for the equivalence of mean-subtracted DMD and DFT ([Theorem 4.1](#)). Using this geometric condition, we construct counterexamples to show that the sufficient condition in [7] is not a necessary condition ([Theorem 4.2](#)).

Then, we proceed to our primary contribution in [Theorem 4.3](#) - linear consistency¹ and over-sampling prevent the equivalence of mean-subtracted DMD and DFT. This result can be paraphrased as follows:

THEOREM 1.1. *Suppose we select a finite number of functions from the span of r Koopman eigen-functions with distinct eigenvalues. Say this collection of functions, aka dictionary, is used to observe the underlying discrete-time dynamical system at $n + 1$ sequential time instances, starting at an initial state that does not lie on the zero level set of any of the r eigenfunctions. Let the resulting mean-subtracted DMD eigenvalues be denoted as $\{\tilde{\lambda}_i\}_{i=1}^n$.*

If the time sequential observations are linearly consistent ([Definition 3.11](#)) and there are more DMD eigenvalues (n) than Koopman eigenvalues (r), then, mean-subtracted DMD is not a temporal DFT.

$$\text{Linear consistency} \ \& \ n \geq r + 1 \implies \{\tilde{\lambda}_i\}_{i=1}^n \neq \{z \neq 1 \mid z^{n+1} = 1\}.$$

By the contrapositive, DMD-DFT equivalence can be used to decide if more data is needed to construct an accurate DMD model. Under the stronger condition of Koopman invariant observables, we also show the converse: DMD-DFT equivalence can result from a paucity of data ([Corollary 4.5](#)).

This paper is organized as follows: [Section 2](#) details the notation adopted in this work. [Section 3](#) introduces the Koopman operator ([3.1](#)) and Dynamic Mode Decomposition ([3.2](#)) before reviewing the effect of mean subtraction ([3.3](#)). Drawing on these, [Section 4](#) explores the relationship between mean subtracted DMD and DFT, resulting in an a posteriori check that alerts to data insufficiency. [Section 5](#) sees the numerical verification of all major results on linear time invariant systems (LTIs), the Van der Pol oscillator and the lid-driven cavity at various flow regimes. [Section 6](#) summarizes the findings and points out relevant questions that remain unanswered.

2. Notation. The notation is mostly standard for our primary objects of interest: (finite) sets, vectors and matrices. The elements of an object are written with subscripts that start at 0 or 1. The operation $\#(\cdot)$ returns the number of elements in the argument, as illustrated below. Sets are denoted with upper-case letters and are enclosed by curly braces. For example,

$$L := \{\lambda_i\}_{i=1}^r = \{\lambda_1, \lambda_2, \dots, \lambda_r\} \implies \#(L) = r.$$

¹An appropriate number of time delays [5, 1] can ensure linear consistency.

Vectors are typically in \mathbb{C}^m , labelled with bold-faced lower-case letters and represented as columns:

$$\mathbf{v} = [v_i]_{i=1}^m = \begin{bmatrix} v_1 \\ v_2 \\ \vdots \\ v_m \end{bmatrix} \implies \#(\mathbf{v}) = m.$$

The i -th standard basis vector is denoted as \mathbf{e}_i :

$$\mathbf{e}_1 = \begin{bmatrix} 1 \\ 0 \\ \vdots \\ 0 \end{bmatrix}, \quad \mathbf{e}_2 = \begin{bmatrix} 0 \\ 1 \\ \vdots \\ 0 \end{bmatrix} \quad \text{and} \quad \mathbf{e}_m = \begin{bmatrix} 0 \\ 0 \\ \vdots \\ 1 \end{bmatrix}.$$

Constant vectors (those with only one unique coefficient) are represented by their value in boldface and dimension as a subscript.

$$\mathbf{1}_m = [1]_{i=1}^m.$$

Matrices are in $\mathbb{C}^{m \times n}$, denoted by bold-faced upper-case letters and written as ordered sets of columns.

$$\mathbf{A} = [\mathbf{a}_j]_{j=1}^n = [a_{ij}]_{i,j=1}^{m,n} = \begin{bmatrix} | & | & \cdots & | \\ \mathbf{a}_1 & \mathbf{a}_2 & \cdots & \mathbf{a}_n \\ | & | & \cdots & | \end{bmatrix}.$$

The (Hermitian) transpose of \mathbf{A} is written as $(\mathbf{A}^H) \mathbf{A}^T$. The letter \mathbf{I} is reserved for the identity matrix.

$$\mathbf{I}_n = [\mathbf{e}_j]_{j=1}^n =: [\delta_{ij}]_{i,j=1}^n.$$

Constant matrices are written similar to their vector counterparts:

$$\mathbf{0}_{m \times n} = [\mathbf{0}_m]_{j=1}^n = [0]_{i,j=1}^{m,n}.$$

The expression $\mathbf{T}[\mathbf{c}]$ represents the companion matrix with 1 on the first sub-diagonal and \mathbf{c} as the last column.

$$\mathbf{c} \in \mathbb{C}^n \implies \mathbf{T}[\mathbf{c}] = \begin{bmatrix} & & & c_1 \\ 1 & & & c_2 \\ & 1 & & c_3 \\ & & \ddots & \vdots \\ & & & 1 & c_n \end{bmatrix}.$$

Sub-spaces are written in script. For instance, $\mathcal{R}(\mathbf{Z})$ and $\mathcal{N}(\mathbf{Z})$ denote the column-space and null-space of \mathbf{Z} respectively. Orthogonal projectors play a crucial role in this work. Under the standard inner product on \mathbb{C}^m , $\mathcal{P}_{\mathcal{W}}$ denotes the orthogonal projector onto the subspace \mathcal{W} . If we let \mathbf{A}^\dagger denote the Moore-Penrose pseudo-inverse of \mathbf{A} , we get:

$$\mathcal{P}_{\mathcal{R}(\mathbf{A})} = \mathbf{A}\mathbf{A}^\dagger, \quad \mathcal{P}_{\mathcal{N}(\mathbf{A}^H)} = \mathbf{I} - \mathbf{A}\mathbf{A}^\dagger.$$

3. Preliminaries. We provide an overview of the ideas needed to understand and build upon existing work regarding the effect of mean-subtraction on DMD. We begin with a brief introduction to the Koopman operator (Subsection 3.1) and its approximation via the Dynamic Mode Decomposition (Subsection 3.2). Then, we consider augmenting DMD with a pre-processing step of mean-subtraction and discuss the concomitant issue of DMD-DFT equivalence (Subsection 3.3). Subsequently, to facilitate a more detailed exposition, we introduce several technical constructs, including the notions of linear consistency (Definition 3.11) and over-sampling (Definition 3.9). Finally, we review the most relevant theoretical contribution from [9] (Theorem 3.12), highlight its shortcomings and set the stage for its resolution.

3.1. The Koopman operator. Consider an autonomous discrete time dynamical system in \mathbb{R}^p .

$$(3.1) \quad \mathbf{v}^+ = \Gamma(\mathbf{v}), \quad \mathbf{v} \in \mathbb{R}^p.$$

The map Γ describes how states (individual elements of \mathbb{R}^p) evolve in time- an admittedly geometric description. A complementary perspective is embodied by the so-called Koopman operator which describes the evolution of *functions* on the state-space (aka observables).

DEFINITION 3.1 (Koopman operator [11]). *Suppose \mathcal{H} denotes a vector space of complex-valued functions on \mathbb{R}^p . If \mathcal{H} is closed under composition with Γ i.e.,*

$$\forall \psi \in \mathcal{H}, \quad \psi \circ \Gamma \in \mathcal{H},$$

then, the Koopman operator, U , associated to (3.1) is defined as follows:

$$(3.2) \quad \begin{aligned} U : \mathcal{H} &\rightarrow \mathcal{H} \\ U \circ \psi &:= \psi \circ \Gamma. \end{aligned}$$

The function-space \mathcal{H} is usually infinite-dimensional. Even though this complexity is inherited by the Koopman operator, the saving grace is its' linearity:

$$\begin{aligned} U \circ (\alpha_1 \psi_1 + \alpha_2 \psi_2) &= (\alpha_1 \psi_1 + \alpha_2 \psi_2) \circ \Gamma \\ &= \alpha_1 \underbrace{\psi_1 \circ \Gamma} + \alpha_2 \underbrace{\psi_2 \circ \Gamma} \\ &= \alpha_1 U \circ \psi_1 + \alpha_2 U \circ \psi_2. \end{aligned}$$

Pushing this further, we can look for eigen-functions i.e. functions that are merely scaled under the action of U .

DEFINITION 3.2 (Koopman eigen-functions (KEFs)). *The function ϕ is said to be an eigen-function of the Koopman operator U with eigen-value λ if and only if the following holds:*

$$(3.3) \quad U \circ \phi = \lambda \phi.$$

A most pertinent property is that linearity allows the eigen-functions² of U to describe the evolution of any function in their span. We can formalize such an expansion as follows:

²We assume that the choice of \mathcal{H} is such that non-trivial eigen-functions exist.

DEFINITION 3.3 (Koopman Mode Decomposition (KMD) [16, 14]). *Suppose the function f lies in the span of the Koopman eigen-functions $\{\phi_i\}_{i \in \mathcal{I}}$ with eigen-values $\{\lambda_i\}_{i \in \mathcal{I}}$. Then, there exist numbers $\{c_i\}_{i \in \mathcal{I}}$ such that*

$$f = \sum_{i \in \mathcal{I}} c_i \phi_i.$$

The quantities $\{c_i\}_{i \in \mathcal{I}}$ are termed the Koopman modes of f associated with eigen-values $\{\lambda_i\}_{i \in \mathcal{I}}$. In addition, for any whole number n , the action of the Koopman operator U is given by a super-position of its' actions on the constituent eigen-functions.

$$U^n \circ f = U^n \circ \left(\sum_{i \in \mathcal{I}} c_i \phi_i \right) = \sum_{i \in \mathcal{I}} c_i (U^n \circ \phi_i) = \sum_{i \in \mathcal{I}} c_i \lambda_i^n \phi_i.$$

To paraphrase, the Koopman mode decomposition explains temporal observations of a potentially *nonlinear* process (3.1) through a *super-position* of exponentials. Unsurprisingly, many algorithms have been designed to approximate this spectral expansion, with DMD being the most prominent.

3.2. Dynamic Mode Decomposition. Dynamic Mode Decomposition [20] is an algorithm that takes time-sequential observations and returns estimates of the constituent Koopman eigen-values and modes. The input to DMD is generated by first choosing m observables of interest (collectively referred to as the dictionary), $\{\psi_i\}_{i=1}^m$, evaluating them along an orbit, $\{\Gamma^j(\mathbf{v}_1)\}_{j=0}^n$, and collecting the resulting observations (aka snapshots) as the columns of a matrix \mathbf{Z} :

$$(3.4) \quad \boldsymbol{\psi} := [\psi_i]_{i=1}^m, \quad \mathbf{Z} := [\boldsymbol{\psi}(\Gamma^j(\mathbf{v}_1))]_{j=0}^n.$$

DMD formulates a least squares problem using specific sub-matrices of \mathbf{Z} , uses the result to construct a Companion matrix whose eigen-values approximate those of the Koopman operator and eigen-vectors lead to estimates of the associated Koopman modes- a procedure that is detailed as Algorithm 3.1.

While this approximation has been studied in [15], we work in a much simpler setting that permits the following guarantee purely from linear algebraic arguments:

THEOREM 3.4. *Suppose $\boldsymbol{\psi}$ lies in the non-redundant span of r distinct Koopman eigen-functions (Definition 3.8) and the initial condition \mathbf{v}_1 is spectrally informative (Definition 3.10).*

If the matrix pair (\mathbf{X}, \mathbf{Y}) is linearly consistent (Definition 3.11) and there are at-least as many DMD eigen-values (n) as there are Koopman eigen-values (r), then, the Koopman eigen-values are a subset of the DMD eigen-values:

$$(\mathbf{X}, \mathbf{Y}) \text{ is linearly consistent} \ \& \ n \geq r \implies \{\lambda_i\}_{i=1}^r \subseteq \{\hat{\lambda}_i\}_{i=1}^n.$$

Furthermore, a DMD mode is non-zero if and only if the associated eigen-value lies in the Koopman spectrum. Specifically, if \mathbf{v}_μ is the eigenvector of \mathbf{T}^ corresponding to eigenvalue μ^3 ,*

$$\mathbf{T}^* \mathbf{v}_\mu = \mu \mathbf{v}_\mu,$$

then,

$$\mathbf{X} \mathbf{v}_\mu \neq \mathbf{0} \iff \mu \in \{\lambda_i\}_{i=1}^r.$$

³ μ is a scalar quantity and is not to be confused with the vectorial quantity $\boldsymbol{\mu}$ which is the temporal mean.

Algorithm 3.1 Dynamic Mode Decomposition (DMD)

Input: Time-series data \mathbf{Z} from (3.4).

1: Partition \mathbf{Z} as follows:

$$(3.5) \quad \mathbf{Z} =: [\mathbf{X} \mid \mathbf{z}_{n+1}].$$

2: Find the best approximation of \mathbf{z}_{n+1} in the span of \mathbf{X} .

$$(3.6) \quad \mathbf{c}^*[\mathbf{Z}] := \mathbf{X}^\dagger \mathbf{z}_{n+1}.$$

3: Form the Companion matrix associated to the DMD model $\mathbf{c}^*[\mathbf{Z}]$.

$$(3.7) \quad \mathbf{T}^* := \mathbf{T}(\mathbf{c}^*[\mathbf{Z}])$$

4: Compute the eigenvalues, $\{\hat{\lambda}_i\}_{i=1}^n$, and eigen-vectors, $\{\mathbf{v}_i\}_{i=1}^n$ of \mathbf{T}^* .

$$\mathbf{T}^* \mathbf{v}_i = \hat{\lambda}_i \mathbf{v}_i$$

5: Construct the DMD mode, $\hat{\mathbf{d}}_i$, corresponding to each DMD eigenvalue, $\hat{\lambda}_i$.

$$\hat{\mathbf{d}}_i := \mathbf{X} \mathbf{v}_i.$$

Output: DMD eigen-values, $\{\hat{\lambda}_i\}_{i=1}^n$, and their modes, $\{\hat{\mathbf{d}}_i\}_{i=1}^n$.

A hyper-parameter of DMD that is fundamental to this and subsequent analyses is the number of DMD eigen-values, n . It determines the complexity of the dynamics that can be captured by the DMD model $\mathbf{c}^*[\mathbf{Z}]$ - a property formally recognized as follows:

DEFINITION 3.5 (Order of a DMD model). *Given the time-series data $\mathbf{Z} \in \mathbb{C}^{m \times (n+1)}$, the order or capacity of the resulting DMD model is defined thus:*

$$(3.8) \quad \text{Companion-order}[\mathbf{Z}] := n.$$

3.3. Mean subtracted Dynamic Mode Decomposition (μ DMD). Mean subtraction is a useful pre-processing step for DMD, when the time series, \mathbf{Z} , represents the solution to certain partial differential equations (PDEs) [7]. In this amendment, elaborated here as [Algorithm 3.2](#), one simply removes the temporal mean of \mathbf{Z} from each of its' columns before performing DMD. The upshot of such a pre-processing is that the resulting DMD eigen-values and modes (3.11) can generate forecasts that respect the boundary conditions associated with the underlying PDE.

Yet, this innocuous modification *may* compromise DMD-based estimates of the Koopman spectrum.

LEMMA 3.6. [7] *Consider the analogue of (3.5) for the mean-subtracted time series \mathbf{Z}_{ms} :*

$$(3.12) \quad \mathbf{Z}_{\text{ms}} =: [\mathbf{X}_{\text{ms}} \mid \mathbf{z}_{n+1} - \boldsymbol{\mu}].$$

Algorithm 3.2 Mean-subtracted Dynamic Mode Decomposition (μ DMD)

Input: Time-series data \mathbf{Z} from (3.4).

- 1: Compute the temporal mean, $\boldsymbol{\mu}$ of the time-series data \mathbf{Z} .

$$(3.9) \quad \boldsymbol{\mu} := \frac{1}{n+1} \sum_{i=1}^{n+1} \mathbf{z}_i.$$

- 2: Remove the temporal mean from each snapshot i.e. column of \mathbf{Z} .

$$(3.10) \quad \mathbf{Z}_{\text{ms}} := [\mathbf{z}_j - \boldsymbol{\mu}]_{j=1}^{n+1}.$$

- 3: Use the mean-subtracted data, \mathbf{Z}_{ms} , as the input for DMD (Algorithm 3.1).

$$(3.11) \quad \{\tilde{\lambda}_i\}_{i=1}^n, \{\tilde{\mathbf{d}}_i\}_{i=1}^n \leftarrow \text{DMD}(\mathbf{Z}_{\text{ms}})$$

Output: Mean-subtracted DMD eigen-values, $\{\tilde{\lambda}_i\}_{i=1}^n$, and their modes, $\{\tilde{\mathbf{d}}_i\}_{i=1}^n$.

If \mathbf{X}_{ms} has linearly independent columns, then, the mean-subtracted DMD eigen-values are the $(n+1)$ -th roots of unity, modulo 1.

$$\mathbf{X}_{\text{ms}} \text{ has full column rank} \implies \{\tilde{\lambda}_i\}_{i=1}^n = \{z \neq 1 \mid z^{n+1} = 1\}.$$

There are three concerning aspects of this result:

1. Broad applicability: The requirement of linearly independent columns in \mathbf{X}_{ms} is met when \mathbf{Z} has full column rank, which is often the case when the snapshots are slices of the solution to a PDE.
2. Content independence: The mean-removed DMD eigenvalues are entirely determined by the parameter n and, thus, have no regard for the information contained in \mathbf{Z}_{ms} .
3. Reduction to a Discrete Fourier Transform (DFT): The DMD eigen-values are restricted to be the $(n+1)$ th roots of unity, modulo 1. As a result, the mean-subtracted DMD modes, $\{\tilde{\mathbf{d}}_i\}_{i=1}^n$, coincide with the Fourier modes of the original time-series, \mathbf{Z} .

The last observation above suggests that the restriction of μ DMD eigenvalues, which is described in Lemma 3.6, could be formalized as follows:

DEFINITION 3.7 (DMD-DFT equivalence). *We say that mean-subtracted DMD (Algorithm 3.2) is equivalent to DFT when the eigenvalues output by it coincide with the $(n+1)$ th roots of unity, modulo 1.*

$$\mu\text{DMD} \equiv \text{DFT} \iff \{\tilde{\lambda}_i\}_{i=1}^n = \{z \neq 1 \mid z^{n+1} = 1\}.$$

Since the discovery of DMD-DFT equivalence, alternative variants of DMD have been developed to achieve the goal of mean subtraction (boundary-condition aware model reduction) without inducing DMD-DFT equivalence [7, 9]. Yet, theoretical investigations of this phenomenon, by itself, have been few and far between. We now focus on one such work [9] that stands out in its efforts to clarify DMD-DFT equivalence.

3.3.1. Towards untangling the equivalence of μ DMD to DFT. Hirsch and co-workers [9] provide a clear exposition of the work by Chen et.al. [7] and derive

sufficient conditions for \mathbf{X}_{ms} to be rank defective. Understanding their contributions necessitates the Koopman mode decomposition of ψ be quantified (Definition 3.8). This facilitates comparing the system complexity with the amount of training data (Definition 3.9) and grading the dynamical information contained in the trajectory starting at \mathbf{v}_1 (Definition 3.10). Combining these formalisms with a notion of “ideal” training data (Definition 3.11) underpins the result of Hirsch et.al. (Theorem 3.12) as well as the contributions in this work.

Our primary assumption is that the Koopman mode expansion of ψ be finite.

DEFINITION 3.8 (Dictionary non-redundantly spanned by distinct KEFs). *The dictionary ψ is said to be in the non-redundant span of r distinct KEFs if there exists a collection of Koopman eigen-functions, $\{\phi_i\}_{i=1}^r$, with distinct Koopman eigen-values, $\{\lambda_i\}_{i=1}^r$, such that*

1. *Every component of ψ lies in the span of $\{\phi_i\}_{i=1}^r$.*

$$\phi := [\phi_i]_{i=1}^r \implies \exists \tilde{\mathbf{C}} \in \mathbb{C}^{m \times r} \text{ such that } \psi = \tilde{\mathbf{C}}\phi.$$

2. *The expansion of ψ in terms of ϕ possesses no redundancies.*

$$\forall i, \quad \tilde{\mathbf{C}}\mathbf{e}_i \neq \mathbf{0}.$$

When ψ is non-redundantly spanned by r distinct KEFs, capturing the r concomitant Koopman modes necessitates a minimum model order of r . Now, by Definition 3.5, the model order, n , also quantifies the amount of training data available. Hence, the number of distinct KEFs, r , can be used to score the usefulness of the snapshot matrix, \mathbf{Z} , in building a generalizable model.

DEFINITION 3.9 (Sampling regimes in DMD). *Suppose ψ is non-redundantly spanned by r distinct KEFs. Then, we may grade the (in)sufficiency of the training data, \mathbf{Z} , for imbibing the DMD model, \mathbf{c}^* , with generalizability as follows:*

1. *Under-sampled ($n < r$): The DMD model has insufficient capacity to describe the r -term Koopman mode expansion.*
2. *Well-sampled ($n \geq r$):*
 - (a) *Just-sampled ($n = r$): The DMD model has the exact capacity needed to capture the r distinct Koopman eigen-values.*
 - (b) *Over-sampled ($n \geq r + 1$): The capacity of the DMD model is more than sufficient to represent all r Koopman eigen-values.*

Despite an abundance of training data, DMD can fail to capture all the underlying Koopman modes if the initial condition, \mathbf{v}_1 , lies on the zero level set of any KEF ϕ_i . Such dynamically simple states are excluded by the condition of “spectral informativeness”.

DEFINITION 3.10 (Spectrally informative state). *Suppose ψ is non-redundantly spanned by r distinct KEFs $\{\phi_i\}_{i=1}^r$. Then, the state \mathbf{v} is said to be spectrally informative if it does not lie on the zero level set of any KEF.*

$$\mathbf{v} \text{ is spectrally informative} \iff \forall i, \phi_i(\mathbf{v}) \neq 0.$$

Finally, we introduce a requirement on sub-matrices of \mathbf{Z} that is necessary for the generalizability of DMD.

DEFINITION 3.11 (Linear consistency [24]). *Let \mathbf{Y} denote the sub-matrix of \mathbf{Z} corresponding to the last n columns:*

$$(3.13) \quad \mathbf{Z} =: [\mathbf{z}_1 \quad \mathbf{Y}].$$

The matrix pair (\mathbf{X}, \mathbf{Y}) is said to be linearly consistent if there exists a linear transform \mathbf{A} that maps \mathbf{X} to \mathbf{Y} .

$$(\mathbf{X}, \mathbf{Y}) \text{ is linearly consistent} \iff \exists \mathbf{A} \text{ such that } \mathbf{A}\mathbf{X} = \mathbf{Y}.$$

With this machinery in place, the contribution of [9] that forms the starting point of our work reads thus:

THEOREM 3.12. *Suppose ψ lies in the non-redundant span of r KEFs with distinct eigen-values $\{\lambda_i\}_{i=1}^r$ and the initial condition \mathbf{v}_1 is spectrally informative. Furthermore, assume that one of these eigen-values takes the value of 1, none of them is 0 and the matrix \mathbf{X} has non-zero mean:*

$$1 \in \{\lambda_i\}_{i=1}^r, 0 \notin \{\lambda_i\}_{i=1}^r \ \& \ \mathbf{X}\mathbf{1}_n \neq \mathbf{0}_m.$$

If the matrix pair (\mathbf{X}, \mathbf{Y}) is linearly consistent and the input to DMD is well-sampled, then, the columns of \mathbf{X}_{ms} are not linearly independent.

$$(\mathbf{X}, \mathbf{Y}) \text{ is linearly consistent} \ \& \ n \geq r \implies \mathbf{X}_{\text{ms}} \text{ doesn't have full column rank.}$$

Although this greatly improves our understanding, the story is still incomplete. One cannot infer non-equivalence of mean-subtracted DMD and DFT, from the rank deficiency of \mathbf{X}_{ms} . Specifically, [Theorem 3.12](#), in conjunction with [Lemma 3.6](#), falls short of producing a necessary condition for $\mu\text{DMD} \equiv \text{DFT}$.

We address this shortcoming through a necessary and sufficient condition ([Theorem 4.1](#)) for DMD-DFT equivalence that is weaker than asking for linear independence of the columns of \mathbf{X}_{ms} . Consequently, we can generate concrete examples⁴ where DMD-DFT equivalence is observed despite \mathbf{X}_{ms} possessing linearly dependent columns ([Theorem 4.2](#)).

Nonetheless, a numerical experiment in [Theorem 3.12](#) indicates conditions under which DMD-DFT equivalence is precluded. Indeed, Figure 4a in [9] suggests that a spectrally informative initial condition, well-sampling, linear consistency and non-zero mean may prevent $\mu\text{DMD} \equiv \text{DFT}$.

We formally prove a refined version of this implicit conjecture in [Theorem 4.3](#).

4. Exploring the what and where of DMD-DFT equivalence. We begin by developing a necessary and sufficient condition for the equivalence of mean-subtracted DMD and DFT ([Theorem 4.1](#)). Building on this result, we find that [Lemma 3.6](#) is a stricter sufficient condition for DMD-DFT equivalence and show that its converse does not hold ([Theorem 4.2](#)). Then, we study the relationship between mean-subtracted DMD and temporal DFT as a function of the order⁵ aka capacity of the DMD model. We find that the occurrence of DMD-DFT equivalence is, for all practical purposes, dictated by the model capacity, n , and the number of Koopman modes, r , comprising the DMD observables ψ ([Theorem 4.3](#) and [Corollary 4.5](#)). Finally, we demonstrate that the requirements for the above results -linearly consistent data, and to a lesser extent, a Koopman invariant ψ - can be met in practice using time delay embedding ([Proposition 4.6](#)).

⁴Certain well-characterized linear dynamical systems observed through a tailored dictionary using specific choices of the model order

⁵See [Definition 3.5](#)

4.1. A geometric characterization of DMD-DFT equivalence.

THEOREM 4.1 (A necessary and sufficient condition for DMD-DFT equivalence).

Mean subtracted DMD of \mathbf{Z} is equivalent to temporal DFT if and only if the constant vector is orthogonal to $\mathcal{N}(\mathbf{X}_{\text{ms}})$, that is,

$$\boldsymbol{\mu}\text{DMD} \equiv \text{DFT} \iff \mathcal{P}_{\mathcal{N}(\mathbf{X}_{\text{ms}})}\mathbf{1}_n = 0.$$

Proof. Refer [Appendix D.1](#) □

Thus, DMD-DFT equivalence is ensured when the constant vector has no projection onto $\mathcal{N}(\mathbf{X}_{\text{ms}})$ - A stringent requirement than asking for a full column rank \mathbf{X}_{ms} ⁶. This relaxation guides us towards situations where $\boldsymbol{\mu}\text{DMD} \equiv \text{DFT}$, despite \mathbf{X}_{ms} having linearly dependent columns.

THEOREM 4.2 (Counter-example that disproves the converse of [Lemma 3.6](#)).

Suppose $\boldsymbol{\psi}$ lies in the non-redundant span of r KEFs with distinct eigen-values $\{\lambda_i\}_{i=1}^r$ and the initial condition \mathbf{v}_1 is spectrally informative. Furthermore, assume that none of these eigen-values takes the value of 1 and the model order (n) lies between 2 and r :

$$1 \notin \{\lambda_i\}_{i=1}^r \quad \& \quad 2 \leq n \leq r.$$

Then, there is an explicitly constructible dictionary $\boldsymbol{\psi}$ such that the resulting matrix \mathbf{X}_{ms} possesses linearly dependent columns and, yet, mean-subtracted DMD is rendered equivalent to temporal DFT:

$$\exists \boldsymbol{\psi} \text{ such that } \mathbf{X}_{\text{ms}} \text{ doesn't have full column rank } \& \boldsymbol{\mu}\text{DMD} \equiv \text{DFT}.$$

Proof. Refer [Appendix D.2](#) □

Therefore, rank defectiveness of \mathbf{X}_{ms} does not preclude DMD-DFT equivalence for the time series \mathbf{Z} . It is worth noting that linear inconsistency of (\mathbf{X}, \mathbf{Y}) and limited data are key ingredients in [Theorem 4.2](#). Pursuing this line of thought, we find that the parameter regime where both conditions fail is devoid of DMD-DFT equivalence ([Theorem 4.3](#)).

4.2. Charting the domain of DMD-DFT equivalence. We probe the effect of Companion-order[\mathbf{Z}] i.e. n on DMD-DFT equivalence for the time series \mathbf{Z} . We begin with the data-rich regime ($n > r$) where linear consistency prevents DMD-DFT equivalence.

THEOREM 4.3. *Suppose $\boldsymbol{\psi}$ lies in the non-redundant span of r distinct KEFs and the initial condition \mathbf{v}_1 is spectrally informative.*

If the matrix pair (\mathbf{X}, \mathbf{Y}) is linearly consistent and the input to DMD is over-sampled, then, mean-subtracted DMD is not a temporal DFT.

$$(\mathbf{X}, \mathbf{Y}) \text{ is linearly consistent } \& \ n \geq r + 1 \implies \boldsymbol{\mu}\text{DMD} \not\equiv \text{DFT}.$$

Proof. Refer [Appendix D.4](#) □

Thus, [Theorem 3.12](#) can be extended by mildly strengthening the sampling condition, retaining linear consistency and dropping all other requirements. The contrapositive is of practical interest: Equivalence of mean-subtracted DMD and DFT may indicate a need to acquire more data for a reliable analysis.

⁶[Lemma 3.6](#) can be obtained from [Theorem 4.1](#) by noting that $\mathcal{N}(\mathbf{X}_{\text{ms}}) = 0$ when \mathbf{X}_{ms} has full column rank.

Moving onto the other data regimes ($n \leq r$), we see that the training set is limited and hence must be vigilant to avoid over-fitting. In particular, the notion of linear consistency, while numerically verifiable, may not lead to good generalization. This shortcoming can be addressed if every observable in the dictionary ψ , when acted upon by the Koopman operator U , continues to remain in the span of ψ .

DEFINITION 4.4 (Koopman invariant dictionary). *Suppose we extend [Definition 3.1](#) in the obvious manner to operate on vector-valued observables i.e.,*

$$(4.1) \quad \forall i, \quad (U \circ \psi)_i := \psi_i \circ \Gamma.$$

Then, Koopman invariance of ψ is defined thus:

$$\psi \text{ is Koopman invariant} \iff \exists \mathbf{A} \text{ such that } U \circ \psi = \mathbf{A}\psi.$$

In other words, Koopman invariance of ψ means linear consistency along any trajectory.

Subsequently, we can draw upon [\[7\]](#) to complete the picture on DMD-DFT equivalence.

COROLLARY 4.5. *Suppose ψ lies in the non-redundant span of r KEFs with distinct eigen-values $\{\lambda_i\}_{i=1}^r$ and the initial condition \mathbf{v}_1 is spectrally informative.*

If ψ is also Koopman invariant, then, the following hold in the just and under-sampled regimes:

1. *When $n = r$, mean-subtracted DMD is equivalent to temporal DFT if and only if 1 is not a Koopman eigenvalue.*

$$\text{When } n = r, \quad \mu\text{DMD} \equiv \text{DFT} \iff 1 \notin \{\lambda_i\}_{i=1}^r.$$

2. *When $n < r$ i.e. the system is under-sampled, mean-subtracted DMD is equivalent to temporal DFT.*

$$n < r \implies \mu\text{DMD} \equiv \text{DFT}.$$

Proof. Refer [Appendix D.5](#) □

Thus, we have a complete understanding of DMD-DFT equivalence, as defined in [Definition 3.7](#), when the observables are Koopman invariant. Barring the pragmatically negligible case of just-sampling ($n = r$), under-sampling is necessary and sufficient for the equivalence of DMD and DFT.

4.3. DMD-DFT equivalence and delay embedding. Linear consistency of (\mathbf{X}, \mathbf{Y}) and, to a smaller extent, Koopman invariance of ψ have been vital to our study of DMD-DFT equivalence. While these properties may not always hold, a simple remedy⁷ is to delay embed the training data \mathbf{Z} before performing μ DMD ([Proposition 4.6](#)). This strategy of prefacing [Algorithm 3.2](#) by taking time-delays, dubbed $d\mu$ DMD ([Algorithm 4.1](#)), permits [Theorem 4.3](#) and [Corollary 4.5](#) to be rephrased without drawing upon linear consistency or Koopman invariance ([Corollary 4.9](#)).

4.3.1. Koopman invariance via time delays.

PROPOSITION 4.6. *Suppose the set of observables ψ lies in the non-redundant span of r distinct Koopman eigen-functions. Consider augmenting ψ by taking d time*

⁷Assuming one has enough snapshots at hand.

delays:

$$\boldsymbol{\psi}_{\text{d-delayed}} := \begin{bmatrix} \boldsymbol{\psi} \\ U \circ \boldsymbol{\psi} \\ \vdots \\ U^d \circ \boldsymbol{\psi} \end{bmatrix}.$$

If at least $r - 1$ time delays are taken, then, the augmented dictionary is Koopman invariant.

$$d \geq r - 1 \implies \boldsymbol{\psi}_{\text{d-delayed}} \text{ is Koopman invariant.}$$

Proof. Refer [Appendix D.6](#). \square

Remark 4.7. Although $r - 1$ delays are suggested, $\boldsymbol{\psi}$ may generate a Koopman invariant dictionary with fewer delays. Specifically, vector valued observables (i.e., $m > 1$) may attain Koopman invariance for $d < r - 1$, as described in Lemma C of [\[13\]](#) and refined in Theorem 2 of [\[18\]](#). In contrast, a scalar valued observable needs an absolute minimum of $r - 1$ delays. In the forthcoming analysis, for the sake of simplicity, we use the potentially conservative prescription in [Proposition 4.6](#) to ensure Koopman invariance.

4.3.2. DMD-DFT equivalence under delay embedding. Consider the variant of μ DMD that results from delay-embedding the observables $\boldsymbol{\psi}$ before performing [Algorithm 3.2](#)- a process that is detailed as [Algorithm 4.1](#). Porting our findings on

Algorithm 4.1 Delay-embedded μ DMD ($d\mu$ DMD)

Input: Time-series data \mathbf{Z} from [\(3.4\)](#) and the number of time-delays d .

- 1: Construct the delay-embedded matrix $\mathbf{Z}_{\text{d-delayed}}$ by taking d time-delays of \mathbf{Z} .

$$(4.2) \quad \mathbf{Z}_{\text{d-delayed}} := \begin{bmatrix} \mathbf{z}_1 & \mathbf{z}_2 & \cdots & \mathbf{z}_{n+1-d} \\ \mathbf{z}_2 & \mathbf{z}_3 & \cdots & \mathbf{z}_{n+2-d} \\ \vdots & \vdots & \ddots & \vdots \\ \mathbf{z}_{1+d} & \mathbf{z}_{2+d} & \cdots & \mathbf{z}_{n+1} \end{bmatrix}.$$

- 2: Compute the associated model order,

$$(4.3) \quad \theta := \text{Companion-order}[\mathbf{Z}_{\text{d-delayed}}].$$

- 3: Use the delay-embedded data, $\mathbf{Z}_{\text{d-delayed}}$, as input for [Algorithm 3.2](#).

$$(4.4) \quad \{\check{\lambda}_i\}_{i=1}^\theta, \{\check{\mathbf{d}}_i\}_{i=1}^\theta \longleftarrow \mu\text{DMD}(\mathbf{Z}_{\text{d-delayed}})$$

Output: $d\mu$ DMD eigen-values, $\{\check{\lambda}_i\}_{i=1}^\theta$, and their modes, $\{\check{\mathbf{d}}_i\}_{i=1}^\theta$.

DMD-DFT equivalence to this strategy requires that we extend the notions of under, just and over-sampling to $\mathbf{Z}_{\text{d-delayed}}$. The hyper-parameter, n , which determines the sampling regime in [Algorithms 3.1](#) and [3.2](#), also happens to be the associated model order ([Definition 3.5](#)). This suggests that generalizing the sampling regimes to [Algorithm 4.1](#) should build upon its model order, θ ⁸. In particular, under-sampling would

⁸Which, by [Definition 3.5](#) and [\(4.2\)](#), has a value of $n - d$.

translate to $\theta < r$, just-sampling would mean $\theta = r$ and over-sampling would denote $\theta > r$. Hence, we can clarify the notion of DMD-DFT equivalence for $d\mu\text{DMD}$:

DEFINITION 4.8. *We say that delay-embedded μDMD (Algorithm 4.1) is equivalent to DFT when the eigenvalues output by it coincide with the $(\theta + 1)$ th roots of unity, modulo 1.*

$$d\mu\text{DMD} \equiv \text{DFT} \iff \{\tilde{\lambda}_i\}_{i=1}^\theta = \{z \neq 1 \mid z^{\theta+1} = 1\}.$$

Consequently, the more pragmatic version of Theorem 4.3 and Corollary 4.5, where time delays are used to meet the relatively abstract conditions of linear consistency and Koopman invariance, reads thus:

COROLLARY 4.9. *Suppose ψ lies in the non-redundant span of r KEFs with distinct eigen-values $\{\lambda_i\}_{i=1}^r$ and the initial condition \mathbf{v}_1 is spectrally informative.*

If at least $r - 1$ time delays have been taken, i.e. $d \geq r - 1$, then, $d\mu\text{DMD}$ reduces to a DFT if and only if we are under-sampled or in the just-sampled regime without a Koopman eigenvalue at 1.

$$d\mu\text{DMD} \equiv \text{DFT} \iff (\theta < r) \text{ OR } (\theta = r \ \& \ 1 \notin \{\lambda_i\}_{i=1}^r).$$

To summarize, when Koopman invariant observables are used, oversampling is (practically) necessary and sufficient to preclude the equivalence of mean-subtracted DMD and DFT. The requisite Koopman invariance can be attained by delay embedding the snapshots.

5. Numerical experiments. The guarantees on DMD-DFT equivalence, in Corollary 4.9, can be computationally illustrated and tested⁹, despite being abstract and fragile. The former can be addressed by translating the mathematical statements into concrete computational tasks, and the latter by testing the translated guarantees on an ensemble of trajectories. The resulting framework for numerically probing Corollary 4.9 is first deployed in scenarios where all the attendant conditions are known to be met. Subsequently, we repeat the same experiments in situations where the requisites of Corollary 4.9 may not be met, and draw upon its' contrapositive to generate lower bounds on the number of Koopman modes required to represent the observations.

5.1. Preamble: Translation and trial-by-ensemble.

5.1.1. A computation-friendly recast of Corollary 4.9. Validating Corollary 4.9 requires that we assess its' predictions about the presence or absence of DMD-DFT equivalence, over an appropriate range of model orders. Alas, by Definition 3.7, the associated predictions take the form of set (in)equalities- properties that cannot be reliably discerned when the underlying computations use finite precision arithmetic. So, we leverage Theorem 4.1 to re-phrase those predictions in a numerically tangible fashion, in terms of a real-valued indicator named **Relative distance to DFT**¹⁰. This numerical quantity takes values on the interval $[0, 1]$, with 0 indicating DMD-DFT equivalence and any other value in $(0, 1]$ representing non-equivalence. Consequently, we may recast Corollary 4.9 thus:

⁹All code used in this analysis can found at https://github.com/gowtham-ss-ragavan/mselect_dmd.git

¹⁰For a precise construction, see Definition D.16

COROLLARY 5.1. Suppose ψ lies in the non-redundant span of r KEFs with distinct eigen-values $\{\lambda_i\}_{i=1}^r$ and the initial condition \mathbf{v}_1 is spectrally informative.

If at least $r - 1$ time delays have been taken, i.e. $d \geq r - 1$, then, the indicator **Relative distance to DFT** is completely determined by the sampling regime and spectral content, as detailed in [Table 5.1](#).

TABLE 5.1

Relative distance to DFT as a function of the sampling regime and the presence or absence of a Koopman eigen-value at 1.

Sampling regime	Spectral condition	Relative distance to DFT
$\theta < r$	None	0
$\theta = r$	$1 \notin \{\lambda_i\}_{i=1}^r$	0
	$1 \in \{\lambda_i\}_{i=1}^r$	$(0, 1]$
$\theta > r$	None	$(0, 1]$

5.1.2. Addressing a persistent fragility with ensemble studies. A non-zero value of **Relative distance to DFT** is useless unless it can be distinguished from 0. Even if we do see this happen for a given trajectory, such an observation does not preclude the possibility of poor discernibility for other trajectories.

Consequently, we systematically test [Corollary 5.1](#) for an ensemble of trajectories. For any choice of a dynamical system [\(3.1\)](#), we pick an appropriate range of Companion-orders and $\#[delays]$ in which [Corollary 5.1](#) is to be examined. For each choice of model-order (θ) and delay embedding dimension (d), we compute **Relative distance to DFT** over an ensemble of trajectories and dictionaries.

To see this in detail, suppose θ_{\max} is the maximal Companion-order and d_{\max} the largest number of time delays to be taken. Consider the trajectory of length $\theta_{\max} + d_{\max} + 1$ beginning at \mathbf{v}_1 and observed through the vector of m observables ψ . The length of the trajectory has been chosen so that we can compute the two numerical indicators for every pair (θ, d) in the entire parameter range. For the choice of (θ, d) , the time series matrix \mathbf{Z} reads thus:

$$(5.1) \quad \mathbf{Z} = [\psi(\mathbf{v}_1) \quad \psi(\Gamma(\mathbf{v}_1)) \quad \dots \quad \psi(\Gamma^{\theta+d}(\mathbf{v}_1))].$$

To paraphrase, \mathbf{Z} corresponds to sampling ψ on the first $\theta + d + 1$ elements of the trajectory. Subsequently, we form $\mathbf{Z}_{d-\text{delayed}}$, perform DMD¹¹ and compute **Relative distance to DFT**. This calculation is, then, iterated over every pair (θ, d) in the parameter regime of interest. Finally, we also repeat this parametric sweep, at a higher level, over many trajectories¹². Consequently, we can study the statistics of **Relative distance to DFT** for every pair of Companion-order (θ) and $\#[delays]$ (d) being tested. This is facilitated by box-whisker plots of this indicator with respect to Companion-order.

We test the major results on a variety of dynamical systems of increasing complexity. We primarily work with linear-time invariant (LTI) systems since their Koopman spectra are easily determined and the conditions required in [Corollary 5.1](#) can be met. We also validate our theory using the Van der Pol oscillator and the lid-driven cavity from [\[2\]](#). In contrast to the LTI systems, we have no guarantee of meeting the requisites in [Corollary 5.1](#) nor do we possess complete knowledge of the associated

¹¹A relative threshold of 10^{-8} is used in all pseudo-inverse computations.

¹²We also switch the dictionary for each trajectory for an added level of randomness.

Koopman spectra. Nonetheless, we can still use the contrapositive of [Corollary 5.1](#) to get a lower bound on the complexity of the underlying Koopman mode expansion.

5.2. Systems satisfying the requisites for [Corollary 5.1](#). Consider the linear time-invariant dynamical system governed by the following update rule:

$$(5.2) \quad \Gamma(\mathbf{v}) := \begin{bmatrix} \lambda_1 & & & \\ & \lambda_2 & & \\ & & \ddots & \\ & & & \lambda_r \end{bmatrix} \mathbf{v}.$$

We set r to be 7 and study three choices of $\{\lambda_i\}_{i=1}^r$, denoted LTI_{1a} , LTI_{1b} and LTI_3 , that are detailed in [Table 5.2](#). For each of these three systems, the Koopman

TABLE 5.2
LTI systems from (5.2) that are used to illustrate [Corollary 5.1](#).

Name	LTI_{1a}	LTI_{1b}	LTI_3
$\{\lambda_i\}_{i=1}^r$	$\{z \mid z^7 = 1\}$	$ \lambda_i = 1, \forall i$	$ \lambda_i = 1, i = 1, 2, 3, 4$ $ \lambda_5 = 0.97, \lambda_6 = 0.93, \lambda_7 = 0.87$

eigenvalues are within the unit disc, but *only* LTI_{1a} possesses a Koopman eigenvalue at 1.

The dynamics specified in (5.2) implies that each individual coordinate function, v_i , is a Koopman eigen-function with eigen-value λ_i . Hence, we have,

$$\phi(\mathbf{v}) = \mathbf{v}.$$

The observable used to study (5.2) is simply a scalar function encoded by an arbitrarily chosen row vector, $\tilde{\mathbf{C}}$, with non-zero entries:

$$\psi := \tilde{\mathbf{C}}\phi.$$

Hence, the dictionary ψ is non-redundantly spanned by r distinct KEFs. Furthermore, we ensure that our choice of initial condition, \mathbf{v}_1 , is always spectrally informative.

Assuming that at-least 6 time delays are taken, [Corollary 5.1](#) makes the following predictions: LTI_{1a} has a Koopman eigenvalue at 1. So, **Relative distance to DFT** will be insignificant when $\theta < 7$ and otherwise for $\theta \geq 7$. The same trend should hold for LTI_{1b} and LTI_3 , with the boundary shifting from 7 to 8 due to the absence of a Koopman eigenvalue at 1.

For the unitary systems LTI_{1a} and LTI_{1b} , the expected trend is clearly visible in sub-figures (a) and (b) of [Figure 5.1](#). **Relative distance to DFT** is orders of magnitude larger when θ crosses the critical value of 7. Moreover, the shadowing of this feature by the pertinent inter-quartile ranges (IQRs), which are denoted by boxes colored according to the number of delays taken, suggests that the observation is independent of the choice of initial condition.

The icing on the cake is that when $\theta = r = 7$, the effect of having $1 \in \{\lambda_i\}_{i=1}^r$ is in concordance with [Corollary 5.1](#). The system LTI_{1b} , which does not have a Koopman eigenvalue at 1, has low values of **Relative distance to DFT** indicating DMD-DFT equivalence. To the contrary, LTI_{1a} exhibits a value that is orders of magnitude larger due to the presence of a Koopman eigenvalue at 1.

The computations with LTI_3 are not in exact agreement with the theoretical claims, particularly when θ matches r . Recall that [Corollary 5.1](#) predicts the same trend for LTI_3 and LTI_{1b} since neither has a Koopman eigenvalue at 1. In sub-figure (c) of [Figure 5.1](#), we observe that DMD-DFT equivalence appears to hold for θ less than 7 and is absent when θ exceeds 7. However, when θ is 7, we see non-equivalence of mean-subtracted DMD and DFT, in contrary to the theoretical prediction of equivalence. We believe that this is a numerical issue arising from the three Koopman eigenvalues of this system that lie *inside* the unit disc (see [Table 5.2](#)). These eigenvalues degrade the conditioning of $\mathbf{Z}_{d-\text{delayed}}$ ¹³ in [Algorithm 4.1](#) and, thus, perturb [Relative distance to DFT](#).

5.3. Systems that *may not be* satisfying the requisites for [Corollary 5.1](#).

When the assumptions (3.8) and (3.10) are not known to hold, we can still use the contrapositive of [Corollary 5.1](#) to provide a lower bound on the number of Koopman modes constituting our dictionary ψ . First, we note that if the predictions of [Corollary 5.1](#) are inconsistent with a numerical study that has taken sufficient time delays, then, at-least one of the assumptions (3.8) and (3.10) must be invalid. In practice, (3.10) holds true because we can restrict our attention to only those KEFs whose zero level set does not contain \mathbf{v}_1 . This change of perspective is permissible because the reduced collection of KEFs is equally capable of generating the training set, \mathbf{Z} , through time-sequential observations. Since (3.8) can be interpreted as requiring ψ possess only r Koopman modes, its negation, over the specific guesses of r described below, can give a lower bound on the number of Koopman modes comprising ψ . Thus, when the delay embedding dimension, d , is large enough, numerical observations of [Relative distance to DFT](#) that are inconsistent with [Corollary 5.1](#) can inform the number of Koopman modes *necessary* to represent ψ .

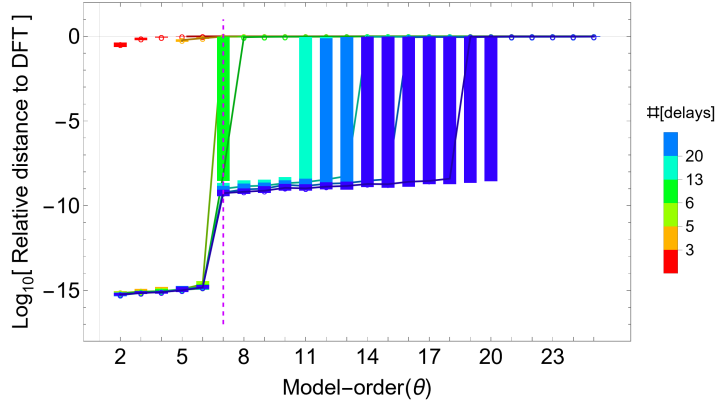
The contrapositive of [Corollary 5.1](#) can be computationally leveraged by assuming an upper-bound on the number of Koopman modes, performing the ensemble experiment described in [Subsection 5.1.2](#) and using errors, if any, in the predictions of [Corollary 5.1](#) to negate the presumed upper-bound. In each forthcoming numerical experiment, we begin with the assumption that our observables are non-redundantly spanned by r distinct KEFs. Although r is unknown, we assume that it is finite and has a known upper bound of r_{\max} . This may be a theoretically informed cap or, if little is known about the system, simply the maximum model order that is palatable from a modeling perspective. Suppose we take at least $r_{\max} - 1$ time delays i.e., $d \geq r_{\max} - 1$. Then, by [Corollary 5.1](#), [Relative distance to DFT](#) must behave like a step function with respect to the model order (θ). It must be near zero for model orders less than $r + 1$ (r if 1 is a Koopman eigenvalue) and significantly higher for larger model orders. The absence of a step-like behavior for θ less than or equal to $r_{\max} + 1$ would, then, mean that at-least $r_{\max} + 1$ distinct KEFs are required to represent the span of our observables i.e., ψ has at-least $r_{\max} + 1$ Koopman modes. In contrast, the presence of a step-like behavior, in agreement with [Corollary 5.1](#), cannot be used to infer that ψ has a finite Koopman mode expansion.

5.3.1. Van der Pol oscillator. We begin with the Van der Pol oscillator, which is defined by the following¹⁴ differential equation:

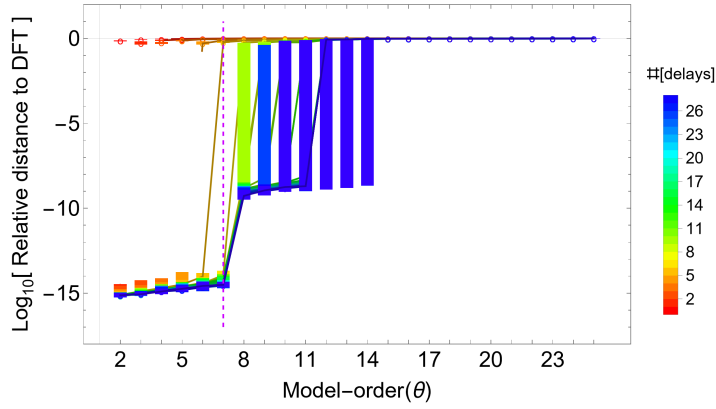
$$(5.3) \quad \begin{aligned} \dot{v}_1 &= v_2 \\ \dot{v}_2 &= (1 - v_1^2)v_2 - v_1. \end{aligned}$$

¹³As compared to its realizations for LTI_{1a} and LTI_{1b}

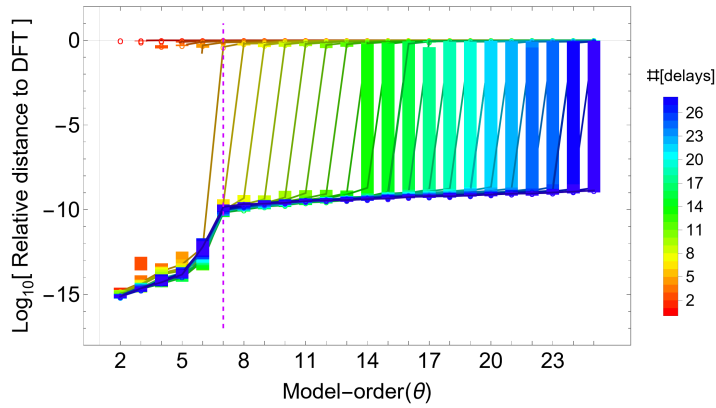
¹⁴ v_1 and v_2 are components of the state \mathbf{v} .



(a) LTI_{1a}



(b) LTI_{1b}



(c) LTI_3

FIG. 5.1. For the linear time-invariant (LTI) systems described by (5.2), box plots of *Relative distance to DFT* reveal its dependence on the model order (θ) and the number of time delays (Colour-coded). The magenta line indicates the system order r , which is 7 for all three examples. When at least 6 time delays are taken, LTI_{1a} (LTI_{1b}) displays a plateau starting at a Companion-order of 7 (8) as predicted by *Corollary 5.1*. Although this plateau begins earlier than expected (at $\theta = 7$ instead of $\theta = 8$) for LTI_3 , the overall trend conforms to the theoretical prediction of *Corollary 5.1*.

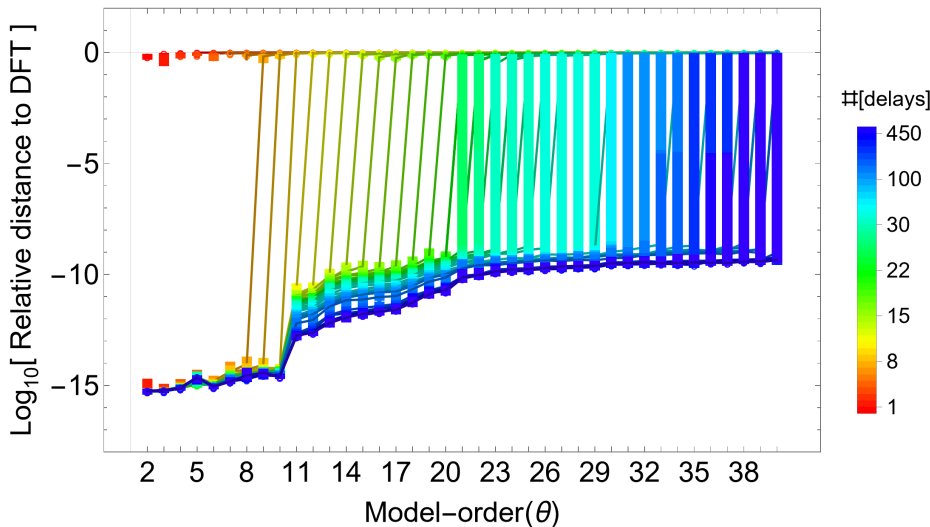


FIG. 5.2. The system order, r , is unknown for the dictionary, ψ , that is used (5.4) to study the Van der Pol oscillator (5.3). Nonetheless, sufficient time delays lead to a step-like trend in Relative distance to DFT. By Corollary 5.1, the location of the jump might be indicative of ψ possessing no more than 11 Koopman modes.

We sample the flow map of (5.3) at equi-spaced points in time to produce the discrete time system (3.1). We choose our observable as an arbitrary but known linear combination of the state:

$$(5.4) \quad \psi[v] := \tilde{C}v, \quad \tilde{C} \in \mathbb{C}^{1 \times 2}.$$

Checking Corollary 5.1 for this system generates Figure 5.2, where taking at-least 15 time delays seems to produce a consistent step-like trend. In particular, the jump in Relative distance to DFT occurs when θ increases from 10 to 11. Hence, ψ might not possess more than 11 Koopman modes. Unfortunately, this speculation cannot be turned into a guarantee using Corollary 5.1.

5.3.2. Lid-driven cavity. Consider the lid-driven cavity for Reynolds numbers (Re) between 13×10^3 and 30×10^3 . As Re increases, the fluid flow transitions from periodic to chaotic, passing through quasi-periodic and mixed behavior [2]. We sample the continuous-time evolution¹⁵ of the lid-driven cavity at equi-spaced points in time to produce the discrete-time dynamics (3.1). We also choose an arbitrary linear functional of an associated stream-function as our observable. This sets the stage to study DMD-DFT equivalence, over a range of model orders (θ) and delay embedding dimension (d).

Over the range of Re considered, the qualitative change in dynamics is reflected in the relationship between Relative distance to DFT and θ (Figure 5.3). As the Reynolds number increases, we see that the step-like trend has its jump smeared out over a wider range of θ . The plateau begins at larger values of θ before disappearing altogether in the last scenario ($Re = 30 \times 10^3$). Hence, our observable may have a finite number of Koopman modes in the first three cases ($Re = 13 \times 10^3$, 16×10^3 and 20×10^3).

¹⁵Numerical simulations from [2].

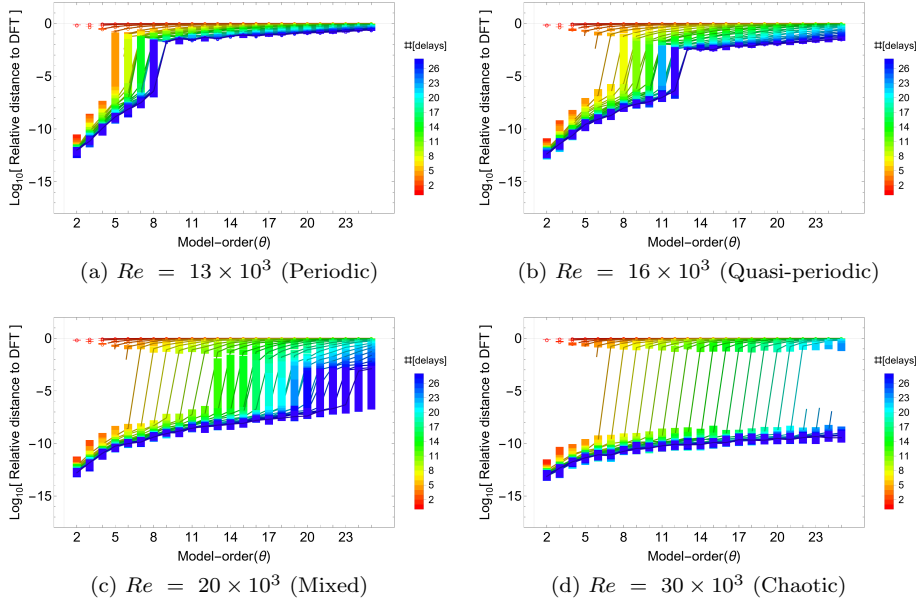


FIG. 5.3. As Re increases, the lid-driven cavity flow grows in complexity. This correlation is reflected in the above box plots of *Relative distance to DFT*. Panels (a)-(c) display jumps that occur at larger values of θ . Furthermore, such jumps are eventually robust to the number of delays. According to [Corollary 5.1](#), such a trend may be the result of an increase in the number of Koopman modes that comprise the observable ψ . In contrast, the final plot (d) is conspicuous in its lack of a discontinuity. By [Corollary 5.1](#), we can infer that ψ possesses at-least 25 Koopman modes. This observation agrees with the fact that the Koopman operator does not possess any eigenfunctions when the underlying dynamics is chaotic.

However, for $Re = 30 \times 10^3$, we can go further and certify that our observable, ψ , possesses at least 25 Koopman modes. To get this guarantee, we first assume that ψ has utmost 24 Koopman modes or, equivalently, that it lies in the span of utmost 24 KEFs. In other words, we assume $r_{\max} = 24$. The concomitant requirement of at least 23 delays is met by the study corresponding to the dark blue boxes in panel (d) of [Figure 5.3](#). Hence, by [Corollary 5.1](#), we would expect it to spike, at the latest, by $\theta = 25$. In contrast to studies with a lower number of time delays, the trend shown by the dark blue boxes lacks a jump. Hence, ψ cannot have fewer than 25 Koopman modes.

Therefore, [Corollary 5.1](#) can provide a data-driven lower bound on the number of Koopman modes of ψ . This is accomplished by taking a minimum number of time delays and looking for *discrepancies* with the predictions made in [Corollary 5.1](#). Alas, one cannot use the confirmation of the same predictions to certify that ψ possesses a finite Koopman mode expansion.

6. Conclusions and Future Work. The relation between mean-subtracted DMD and temporal DFT has been clarified, for observables that possess only a finite number of Koopman modes. When a collection of such observables spans a subspace invariant under the Koopman operator and is chosen as the dictionary in DMD, non-equivalence of mean-subtracted DMD and DFT is tantamount to sufficiency of training data. The requisite invariance can be attained by taking as many time delays as the number of distinct Koopman modes. Therefore, DMD-DFT equivalence

vanishes when data is plentiful, and delay embedded. The contrapositive suggests that DMD-DFT equivalence can be used as an indicator of inadequate training data—a property that contrasts with its’ original perception as a potential rot.

For future work, we note that increasing the number of time delays, far beyond the prescription of [Proposition 4.6](#), distributes the departure from DMD-DFT equivalence over two jumps. The theory developed in this work remains confined to predicting the first jump. Understanding the second jump along with the robustness of the overall transition to conditioning will improve the reliability of DMD-DFT equivalence in inferring the order of the underlying dynamics.

Acknowledgments. This work was supported by the Army Research Office (ARO-MURI W911NF-17-1-030) and the National Science Foundation (Grant no. 1935327).

REFERENCES

- [1] H. ARBABI AND I. MEZIC, *Ergodic theory, dynamic mode decomposition, and computation of spectral properties of the koopman operator*, SIAM Journal on Applied Dynamical Systems, 16 (2017), pp. 2096–2126.
- [2] H. ARBABI AND I. MEZIC, *Spectral analysis of mixing in 2d high-reynolds flows*, arXiv preprint arXiv:1903.10044, (2019).
- [3] A. AVILA AND I. MEZIĆ, *Data-driven analysis and forecasting of highway traffic dynamics*, Nature communications, 11 (2020), pp. 1–16.
- [4] B. W. BRUNTON, L. A. JOHNSON, J. G. OJEMANN, AND J. N. KUTZ, *Extracting spatial–temporal coherent patterns in large-scale neural recordings using dynamic mode decomposition*, Journal of neuroscience methods, 258 (2016), pp. 1–15.
- [5] S. L. BRUNTON, B. W. BRUNTON, J. L. PROCTOR, E. KAISER, AND J. N. KUTZ, *Chaos as an intermittently forced linear system*, Nature communications, 8 (2017), pp. 1–9.
- [6] S. L. BRUNTON, M. BUDIŠIĆ, E. KAISER, AND J. N. KUTZ, *Modern koopman theory for dynamical systems*, arXiv preprint arXiv:2102.12086, (2021).
- [7] K. K. CHEN, J. H. TU, AND C. W. ROWLEY, *Variants of dynamic mode decomposition: Boundary condition, koopman, and fourier analyses*, Journal of Nonlinear Science, 22 (2012), pp. 887–915.
- [8] J. P. HESPANHA, *Linear systems theory*, Princeton university press, 2018.
- [9] S. M. HIRSH, K. D. HARRIS, J. N. KUTZ, AND B. W. BRUNTON, *Centering data improves the dynamic mode decomposition*, SIAM Journal on Applied Dynamical Systems, 19 (2020), pp. 1920–1955.
- [10] R. A. HORN AND C. R. JOHNSON, *Matrix analysis*, Cambridge university press, 2012.
- [11] B. O. KOOPMAN, *Hamiltonian systems and transformation in hilbert space*, Proceedings of the National Academy of Sciences of the United States of America, 17 (1931), p. 315.
- [12] M. KORDA AND I. MEZIĆ, *On convergence of extended dynamic mode decomposition to the koopman operator*, Journal of Nonlinear Science, 28 (2018), pp. 687–710.
- [13] S. LE CLAINCHE AND J. M. VEGA, *Higher order dynamic mode decomposition*, SIAM Journal on Applied Dynamical Systems, 16 (2017), pp. 882–925.
- [14] I. MEZIĆ, *Spectral properties of dynamical systems, model reduction and decompositions*, Nonlinear Dynamics, 41 (2005), pp. 309–325.
- [15] I. MEZIC, *On numerical approximations of the koopman operator*, arXiv preprint arXiv:2009.05883, (2020).
- [16] I. MEZIĆ AND A. BANASZUK, *Comparison of systems with complex behavior*, Physica D: Nonlinear Phenomena, 197 (2004), pp. 101–133.
- [17] S. E. OTTO AND C. W. ROWLEY, *Koopman operators for estimation and control of dynamical systems*, Annual Review of Control, Robotics, and Autonomous Systems, 4 (2021), pp. 59–87.
- [18] S. PAN AND K. DURAISAMY, *On the structure of time-delay embedding in linear models of non-linear dynamical systems*, Chaos: An Interdisciplinary Journal of Nonlinear Science, 30 (2020), p. 073135.
- [19] J. L. PROCTOR AND P. A. ECKHOFF, *Discovering dynamic patterns from infectious disease data using dynamic mode decomposition*, International health, 7 (2015), pp. 139–145.
- [20] C. W. ROWLEY, I. MEZIĆ, S. BAGHERI, P. SCHLATTER, AND D. S. HENNINGSON, *Spectral*

- analysis of nonlinear flows*, Journal of Fluid Mechanics, 641 (2009), pp. 115–127.
- [21] S. SARMAST, R. DADFAR, R. F. MIKKELSEN, P. SCHLATTER, S. IVANELL, J. N. SØRENSEN, AND D. S. HENNINGSON, *Mutual inductance instability of the tip vortices behind a wind turbine*, Journal of Fluid Mechanics, 755 (2014), pp. 705–731.
- [22] P. J. SCHMID, *Dynamic mode decomposition of numerical and experimental data*, Journal of Fluid Mechanics, 656 (2010), pp. 5–28.
- [23] P. J. SCHMID, *Dynamic mode decomposition and its variants*, Annual Review of Fluid Mechanics, 54 (2022), pp. 225–254.
- [24] J. H. TU, C. W. ROWLEY, D. M. LUCHTENBURG, S. L. BRUNTON, AND J. N. KUTZ, *On dynamic mode decomposition: Theory and applications*, arXiv preprint arXiv:1312.0041, (2013).
- [25] M. O. WILLIAMS, I. G. KEVREKIDIS, AND C. W. ROWLEY, *A data-driven approximation of the koopman operator: Extending dynamic mode decomposition*, Journal of Nonlinear Science, 25 (2015), pp. 1307–1346.

Appendix A. Unpacking the structure induced by Definitions 3.8 and 3.10. ■

All the major results in this work make the following two assumptions:

1. The dictionary ψ lies in the non-redundant span of r KEFs, $\{\phi_i\}_{i=1}^r$, with distinct eigenvalues, $\{\lambda_i\}_{i=1}^r$ (Definition 3.8).
2. The initial condition \mathbf{v}_1 is spectrally informative (Definition 3.10).

In this setting, the Koopman mode expansion of ψ (Definition 3.3) manifests as a specific factorization of the time series \mathbf{Z} (Appendix A.1). Furthermore, one of these factors, the matrix of Koopman modes, provides an alternative characterization of the Koopman invariance (Definition 4.4) of ψ (Appendix A.2).

A.1. The Koopman mode factorization of \mathbf{Z} .

LEMMA A.1. *Suppose ψ lies in the non-redundant span of r KEFs, $\{\phi_i\}_{i=1}^r$, with distinct eigenvalues, $\{\lambda_i\}_{i=1}^r$.*

Then, the row-space of \mathbf{Z} is contained in the row space of the Vandermonde matrix,

$$(A.1) \quad \Theta := \begin{bmatrix} 1 & \lambda_1 & \lambda_1^2 & \dots & \lambda_1^n \\ 1 & \lambda_2 & \lambda_2^2 & \dots & \lambda_2^n \\ \vdots & \vdots & \vdots & \ddots & \vdots \\ 1 & \lambda_r & \lambda_r^2 & \dots & \lambda_r^n \end{bmatrix}.$$

Specifically, if we define \mathbf{C} to be the column scaling of $\tilde{\mathbf{C}}$ (3.8) by the eigen-coordinates of the initial condition \mathbf{v}_1 ,

$$(A.2) \quad \text{diag}[\phi(\mathbf{v}_1)] := \begin{bmatrix} \phi_1(\mathbf{v}_1) & & & & \\ & \phi_2(\mathbf{v}_1) & & & \\ & & \ddots & & \\ & & & \ddots & \\ & & & & \phi_r(\mathbf{v}_1) \end{bmatrix}, \quad \mathbf{C} := \tilde{\mathbf{C}} \text{diag}[\phi(\mathbf{v}_1)],$$

we get a “Koopman mode” factorization of \mathbf{Z} :

$$(A.3) \quad \mathbf{Z} = \mathbf{C}\Theta.$$

Furthermore, a spectrally informative \mathbf{v}_1 is necessary and sufficient to ensure there are no redundancies in said decomposition:

$$(A.4) \quad \mathbf{v}_1 \text{ is spectrally informative} \iff \forall i, \quad \mathbf{C}\mathbf{e}_i \neq \mathbf{0}.$$

Proof. We begin with the definition of \mathbf{Z} in (3.4):

$$\mathbf{z}_j = \psi(\Gamma^j(\mathbf{v}_1)).$$

Using [Definition 3.8](#), if we write ψ in terms of the eigenfunctions ϕ , then, the potentially nonlinear map Γ^j can be replaced with the Koopman operator ([Definition 3.1](#) and [\(4.1\)](#)).

$$\underbrace{\psi}_{\Gamma^j(\mathbf{v}_1)} = \tilde{\mathbf{C}} \left(\underbrace{\phi \circ \Gamma^j}_{\phi \circ \Gamma^j} \right) (\mathbf{v}_1) = \tilde{\mathbf{C}} (U^j \circ \phi) (\mathbf{v}_1).$$

If we unpack each component of $(U^j \circ \phi) (\mathbf{v}_1)$ and invoke [Definition 3.2](#),

$$(U^j \circ \phi) (\mathbf{v}_1) = \left[\left(\underbrace{U^j \circ \phi_i}_{U^j \circ \phi_i} \right) (\mathbf{v}_1) \right]_{i=1}^r = \left[\lambda_i^j \phi_i(\mathbf{v}_1) \right]_{i=1}^r,$$

then, we can use [\(A.2\)](#) to replace $\tilde{\mathbf{C}}$ with \mathbf{C} .

$$\tilde{\mathbf{C}} \left[\lambda_i^j \phi_i(\mathbf{v}_1) \right]_{i=1}^r = \underbrace{\tilde{\mathbf{C}} \text{diag}[\phi(\mathbf{v}_1)]}_{\tilde{\mathbf{C}} \text{diag}[\phi(\mathbf{v}_1)]} \left[\lambda_i^j \right]_{i=1}^r = \mathbf{C} \left[\lambda_i^j \right]_{i=1}^r.$$

Compiling this expression for each column of \mathbf{Z} gives [\(A.3\)](#). Lastly, [Definition 3.10](#) and [\(A.2\)](#), when taken together, readily yield [\(A.4\)](#). \square

Remark A.2. If we define Θ_j as Θ without the last j columns,

$$(A.5) \quad \Theta_j := \begin{bmatrix} 1 & \lambda_1 & \lambda_1^2 & \dots & \lambda_1^{n-j} \\ 1 & \lambda_2 & \lambda_2^2 & \dots & \lambda_2^{n-j} \\ \vdots & \vdots & \vdots & \ddots & \vdots \\ 1 & \lambda_r & \lambda_r^2 & \dots & \lambda_r^{n-j} \end{bmatrix},$$

and denote by Λ an appropriate diagonal matrix of Koopman eigenvalues,

$$(A.6) \quad \Lambda := \begin{bmatrix} \lambda_1 & & & & \\ & \lambda_2 & & & \\ & & \ddots & & \\ & & & \ddots & \\ & & & & \lambda_r \end{bmatrix},$$

then, an analogue of [\(A.3\)](#) exists for the sub-matrices \mathbf{X} and \mathbf{Y} too:

$$(A.7) \quad \begin{aligned} \mathbf{X} &= [\mathbf{z}_j]_{j=0}^{n-1} = \mathbf{C}\Theta_1. \\ \mathbf{Y} &= [\mathbf{z}_j]_{j=1}^n = \mathbf{C}\Lambda\Theta_1. \end{aligned}$$

A.2. An analytically useful re-phrasal of Koopman invariance.

PROPOSITION A.3. *Suppose ψ lies in the non-redundant span of distinct KEFs. Then, Koopman invariance of ψ is equivalent to the columns of $\tilde{\mathbf{C}}$ being linearly independent.*

$$(A.8) \quad \psi \text{ is Koopman invariant} \iff \tilde{\mathbf{C}} \text{ has full column rank.}$$

Under the additional condition of a spectrally informative \mathbf{v}_1 , Koopman invariance can be inferred, alternatively, from the matrix \mathbf{C} :

$$(A.9) \quad \psi \text{ is Koopman invariant} \iff \mathbf{C} \text{ has full column rank.}$$

Proof. We will focus on establishing (A.8) since it readily leads¹⁶ to (A.9). We begin with the backward implication. Consider the $m \times m$ matrix,

$$\mathbf{A} := \tilde{\mathbf{C}}\mathbf{\Lambda}\tilde{\mathbf{C}}^\dagger,$$

where $\mathbf{\Lambda}$ is from (A.6). We will show that $U \circ \psi = \mathbf{A}\psi$, by expanding ψ on the right-hand side using Definition 3.8 and, then, unpacking \mathbf{A} :

$$\mathbf{A} \underbrace{\psi} = \underbrace{\mathbf{A}} \tilde{\mathbf{C}}\phi = (\tilde{\mathbf{C}}\mathbf{\Lambda}\tilde{\mathbf{C}}^\dagger)\tilde{\mathbf{C}}\phi.$$

Since $\tilde{\mathbf{C}}$ has full column rank, $\tilde{\mathbf{C}}^\dagger\tilde{\mathbf{C}} = \mathbf{I}$. Using this identity lets us apply (4.1) and (A.6) simultaneously to bring in the Koopman operator U :

$$\tilde{\mathbf{C}}\mathbf{\Lambda}\underbrace{\tilde{\mathbf{C}}^\dagger\tilde{\mathbf{C}}}\phi = \tilde{\mathbf{C}}\underbrace{\mathbf{\Lambda}}\phi = \tilde{\mathbf{C}}(U \circ \phi).$$

Finally, we can use the linearity of U to link $\tilde{\mathbf{C}}$ and ϕ :

$$\underbrace{\tilde{\mathbf{C}}}_{U \circ \phi} = U \circ \underbrace{\tilde{\mathbf{C}}\phi} = U \circ \psi.$$

For the forward implication, recall that a Koopman invariant ψ implies, by Definition 4.4, the existence of a matrix \mathbf{A} such that

$$U \circ \psi = \mathbf{A}\psi.$$

Now, for the left-hand side, we can simply reverse the steps taken towards the conclusion of the forward implication- Invoke Definition 3.8, follow it up with the linearity of U and conclude by applying (4.1) and (A.6) simultaneously:

$$U \circ \underbrace{\psi} = \underbrace{U \circ \tilde{\mathbf{C}}\phi} = \tilde{\mathbf{C}}\underbrace{U \circ \phi} = \tilde{\mathbf{C}}\mathbf{\Lambda}\phi.$$

For the right-hand side, simply apply Definition 3.8.

$$\mathbf{A} \underbrace{\psi} = \mathbf{A}\tilde{\mathbf{C}}\phi.$$

Combining the two expansions, we get:

$$\tilde{\mathbf{C}}\mathbf{\Lambda}\phi = \mathbf{A}\tilde{\mathbf{C}}\phi.$$

Since this relationship holds for all values of ϕ , we have:

$$\tilde{\mathbf{C}}\mathbf{\Lambda} = \mathbf{A}\tilde{\mathbf{C}}.$$

Observe that, by (A.6), the columns of $\tilde{\mathbf{C}}$ are the eigen vectors of \mathbf{A} corresponding to distinct eigen-values. Hence, they must be linearly independent. \square

Appendix B. The size of a Vandermonde matrix can determine its rank.

Vandermonde matrices will be ubiquitous in the forthcoming analysis. In preparation, we highlight two rank conditions, using the Vandermonde matrix,

$$(B.1) \quad \mathbf{V} := \begin{bmatrix} 1 & \nu_1 & \nu_1^2 & \dots & \nu_1^{c-1} \\ 1 & \nu_2 & \nu_2^2 & \dots & \nu_2^{c-1} \\ \vdots & \vdots & \vdots & \ddots & \vdots \\ 1 & \nu_r & \nu_r^2 & \dots & \nu_r^{c-1} \end{bmatrix}.$$

The r complex numbers $\{\nu_i\}_{i=1}^r$, whose powers constitute \mathbf{V} , are called its ‘‘nodes’’.

¹⁶When combined with Definition 3.10 and (A.2).

LEMMA B.1 (Node distinctness lets size dictate rank). [10, 9] Suppose the nodes of \mathbf{V} are distinct:

$$\forall (i, j), \quad i \neq j \implies v_i \neq v_j.$$

Then, either the rows or the columns of \mathbf{V} are linearly independent:

$$(B.2) \quad \mathbf{V} \text{ has full row rank} \iff r \leq c,$$

$$(B.3) \quad \mathbf{V} \text{ has full column rank} \iff c \leq r.$$

Appendix C. On approximating the Koopman eigen-values via DMD.

Under the assumptions (3.8) and (3.10), we prove that linearly consistent and well-sampled training data produces DMD eigen-values, $\{\hat{\lambda}_i\}_{i=1}^n$, that contain the true Koopman eigen-values, $\{\lambda_i\}_{i=1}^r$. Furthermore, the latter are characterized by the corresponding DMD modes being non-zero.

We begin by generalizing an existence result from [18], where it is unduly restricted to roots of unity, to allow for arbitrary and distinct eigen-values:

PROPOSITION C.1. Suppose (3.8) is true. If the DMD problem is well-sampled, then, the last snapshot, \mathbf{z}_{n+1} , is a linear combination of the preceding snapshots.

$$n \geq r \implies \mathbf{z}_{n+1} \in \mathcal{R}(\mathbf{X}).$$

Proof. We can simply recast the arguments used in Theorem 1 of [18], using the machinery developed so far. According to (B.2) and (B.3), the condition $n \geq r$ ensures that the last column of Θ lies in the span of Θ_1 i.e.,

$$\Theta \mathbf{e}_{n+1} \in \mathcal{R}(\Theta_1).$$

If we pre-multiply both sides with \mathbf{C} , then, we can apply (A.3) and (A.7) to reach the desired conclusion. \square

Next, we leverage linear consistency and well-sampling to comment on $\tilde{\mathbf{C}}$.

PROPOSITION C.2. Suppose (3.8) and (3.10) are true. If (\mathbf{X}, \mathbf{Y}) is linearly consistent and the DMD problem is well-sampled, then, the columns of $\tilde{\mathbf{C}}$ are linearly independent.

$$(\mathbf{X}, \mathbf{Y}) \text{ is linearly consistent} \ \& \ n \geq r \implies \tilde{\mathbf{C}} \text{ has full column rank.}$$

Proof. Linear consistency of (\mathbf{X}, \mathbf{Y}) , by Definition 3.11, implies there exists a matrix \mathbf{A} such that $\mathbf{A}\mathbf{X} = \mathbf{Y}$. We may expand the data matrices using (A.7) to obtain:

$$\mathbf{A} \underbrace{\mathbf{X}} = \underbrace{\mathbf{Y}} \iff (\mathbf{A}\mathbf{C})\Theta_1 = (\mathbf{C}\Lambda)\Theta_1.$$

The dependence on the initial condition \mathbf{v}_1 can be factored out using the definition of \mathbf{C} (A.2) together with the fact that Λ and $\text{diag}[\phi(\mathbf{v}_1)]$ commute:

$$\begin{aligned} \mathbf{A} \underbrace{\mathbf{C}} \Theta_1 &= \mathbf{A} \tilde{\mathbf{C}} \text{diag}[\phi(\mathbf{v}_1)] \Theta_1, \\ \underbrace{\mathbf{C}} \Lambda \Theta_1 &= \tilde{\mathbf{C}} \underbrace{\text{diag}[\phi(\mathbf{v}_1)] \Lambda} \Theta_1 = (\tilde{\mathbf{C}}\Lambda) \text{diag}[\phi(\mathbf{v}_1)] \Theta_1. \end{aligned}$$

Combining these results, we have:

$$(C.1) \quad (\mathbf{A}\tilde{\mathbf{C}} - \tilde{\mathbf{C}}\Lambda) \text{diag}[\phi(\mathbf{v}_1)] \Theta_1 = \mathbf{0}.$$

The matrix $\text{diag}[\phi(\mathbf{v}_1)]\Theta_1$ has full row rank. To see this, we may first use \mathbf{v}_1 being spectrally informative (3.10) alongside (A.2) to infer that $\text{diag}[\phi(\mathbf{v}_1)]$ is invertible. Then, we can consider the $r \times n$ Vandermonde matrix Θ_1 . Since it has distinct nodes, well-sampling ($n \geq r$) lets us use (B.2) to conclude that Θ_1 has linearly independent rows. Since the product of two matrices with full row rank will also have full row rank, we find that the rows of $\text{diag}[\phi(\mathbf{v}_1)]\Theta_1$ are linearly independent. Hence, (C.1) is equivalent to the following identity:

$$(C.2) \quad \mathbf{A}\tilde{\mathbf{C}} = \tilde{\mathbf{C}}\Lambda.$$

By (A.6), Λ is a diagonal matrix constructed by collecting the Koopman eigen-values, $\{\lambda_i\}_{i=1}^r$, which, according to (3.8), are r distinct complex numbers. The resulting re-interpretation of (C.2)- the columns of $\tilde{\mathbf{C}}$ are eigen-vectors of \mathbf{A} corresponding to distinct eigen-values- yields the desired conclusion. \square

With these pieces in place, we can establish the recovery of Koopman eigenvalues via Companion DMD.

Proof of Theorem 3.4. We preface the proof by establishing that \mathbf{C} has full column rank. Firstly, Proposition C.2 tells us that the columns of $\tilde{\mathbf{C}}$ are linearly independent. Building on this, we only need apply (A.2) and (3.10) to show that \mathbf{C} also has full column rank.

Now, consider the least-squares interpretation of (3.6):

$$(C.3) \quad \mathbf{c}^*[\mathbf{Z}] = \mathbf{X}^\dagger \mathbf{z}_{n+1} = \begin{cases} \arg \min_{\mathbf{c}} \|\mathbf{c}\|_2 & \mathbf{z}_{n+1} \in \mathcal{R}(\mathbf{X}) \\ \text{subject to } \mathbf{X}\mathbf{c} = \mathbf{z}_{n+1} & \\ \arg \min_{\mathbf{c}} \|\mathbf{X}\mathbf{c} - \mathbf{z}_{n+1}\|_2 & \text{Otherwise} \end{cases}.$$

Since $n \geq r$, Proposition C.1 tells us that the first branch is active. Hence,

$$\mathbf{X}\mathbf{c}^*[\mathbf{Z}] = \mathbf{z}_{n+1},$$

or equivalently, by (3.7) and the definition of \mathbf{Y} ,

$$\mathbf{X}\mathbf{T}^* = \mathbf{Y}.$$

Now, we can expand both \mathbf{X} and \mathbf{Y} according to (A.7), and then safely discard \mathbf{C} owing to its full column rank:

$$\underbrace{\mathbf{X}} \mathbf{T}^* - \underbrace{\mathbf{Y}} = \mathbf{0} \iff \underbrace{\mathbf{C}} (\Theta_1 \mathbf{T}^* - \Lambda \Theta_1) = \mathbf{0} \iff \Theta_1 \mathbf{T}^* - \Lambda \Theta_1 = \mathbf{0}.$$

Since Λ is a diagonal matrix, the final identity,

$$(C.4) \quad \Theta_1 \mathbf{T}^* = \Lambda \Theta_1,$$

is an eigenvector-eigenvalue equation. The rows of Θ_1 are the left eigenvectors of \mathbf{T}^* with the corresponding eigenvalues on the diagonal of Λ . Hence, by (A.6), we have:

$$(C.5) \quad \{\lambda_i\}_{i=1}^r \subseteq \{\hat{\lambda}_i\}_{i=1}^n.$$

Moving onto the second statement, we can show the forward implication by starting with the definition of \mathbf{v}_μ :

$$\mathbf{T}^* \mathbf{v}_\mu = \mu \mathbf{v}_\mu.$$

If we pre-multiply both sides with Θ_1 , it is possible to apply (C.4):

$$\Theta_1 \mathbf{T}^* \mathbf{v}_\mu = \mu \Theta_1 \mathbf{v}_\mu \implies \Lambda(\Theta_1 \mathbf{v}_\mu) = \mu (\Theta_1 \mathbf{v}_\mu).$$

Now, $\Theta_1 \mathbf{v}_\mu \neq \mathbf{0}$. To see this, start with $\mathbf{X} \mathbf{v}_\mu \neq \mathbf{0}$ and sequentially apply (A.7) followed by the full column rank of \mathbf{C} :

$$\underbrace{\mathbf{X}} \mathbf{v}_\mu \neq \mathbf{0} \iff \underbrace{\mathbf{C}} \Theta_1 \mathbf{v}_\mu \neq \mathbf{0} \iff \Theta_1 \mathbf{v}_\mu \neq \mathbf{0}.$$

Consequently, μ is an eigenvalue of Λ and hence, by (A.6), $\mu \in \{\lambda_i\}_{i=1}^r$.

The backward implication can be established using the duality of the left and right eigenvectors of \mathbf{T}^* . Firstly, we note that (C.5) gives $\mu \in \{\hat{\lambda}_i\}_{i=1}^n$. So, we can let \mathbf{w}_μ denote the¹⁷ normalized left eigenvector of \mathbf{T}^* corresponding to the eigenvalue μ .

$$\mathbf{w}_\mu^T \mathbf{T}^* = \mu \mathbf{w}_\mu^T, \quad \|\mathbf{w}_\mu\|_2 = 1.$$

Then, by duality, we have

$$(C.6) \quad \mathbf{w}_\mu^T \mathbf{v}_\mu \neq 0.$$

Since $\mu \in \{\lambda_i\}_{i=1}^r$, by (C.4), there is a row of Θ_1 that is a scaled version of \mathbf{w}_μ^T . Hence, according to (C.6), we have:

$$\Theta_1 \mathbf{v}_\mu \neq \mathbf{0}.$$

Pre-multiplying both sides with \mathbf{C} shows that the DMD mode corresponding to μ , $\mathbf{X} \mathbf{v}_\mu$, has non-zero norm. \square

Appendix D. On DMD-DFT equivalence.

LEMMA D.1 (A vector equality that encodes μ DMD \equiv DFT). *A necessary and sufficient condition for μ DMD (Algorithm 3.2) to be equivalent¹⁸ to a temporal DFT is that the μ DMD model, $\mathbf{c}^*[\mathbf{Z}_{\text{ms}}]$, coincide with $-\mathbf{1}_n$.*

$$\mu\text{DMD} \equiv \text{DFT} \iff \mathbf{c}^*[\mathbf{Z}_{\text{ms}}] = -\mathbf{1}_n.$$

Proof. By Definition 3.7, we have,

$$\mu\text{DMD} \equiv \text{DFT} \iff \{\tilde{\lambda}_i\}_{i=1}^n = \{z \neq 1 \mid z^{n+1} = 1\}.$$

Since $\{\tilde{\lambda}_i\}_{i=1}^n$ are defined in Algorithm 3.2 to be the eigenvalues of the Companion matrix $\mathbf{T}(\mathbf{c}^*[\mathbf{Z}_{\text{ms}}])$, we have the desired conclusion. \square

D.1. A necessary and sufficient condition.

Proof of Theorem 4.1. The key here is to establish the identity,

$$(D.1) \quad \mathbf{c}^*[\mathbf{Z}_{\text{ms}}] = -\mathcal{P}_{\mathcal{R}(\mathbf{x}_{\text{ms}}^H)}(\mathbf{1}_n),$$

because it reduces, by Lemma D.1, the justification of Theorem 4.1 to an exercise in linear algebra. Indeed, the forthcoming analysis is underpinned by a single linear algebraic identity:

$$(D.2) \quad I = \mathcal{P}_{\mathcal{N}(\mathbf{x}_{\text{ms}})} + \mathcal{P}_{\mathcal{R}(\mathbf{x}_{\text{ms}}^H)}.$$

¹⁷We say “the” and not “a” because companion matrices can only have a single eigenvector for an eigenvalue, regardless of its multiplicity [10].

¹⁸As described in Definition 3.7.

Consider the least-squares problem that is solved in [Algorithm 3.2](#) to build the mean-subtracted DMD model $\mathbf{c}^*[\mathbf{Z}_{\text{ms}}]$:

$$(D.3) \quad \begin{aligned} \mathbf{c}^*[\mathbf{Z}_{\text{ms}}] &= \mathbf{X}_{\text{ms}}^\dagger (\mathbf{z}_{n+1} - \boldsymbol{\mu}) = \arg \min_{\mathbf{c}} \|\mathbf{c}\|_2 \\ &\text{subject to } \mathbf{X}_{\text{ms}} \mathbf{c} = \mathbf{z}_{n+1} - \boldsymbol{\mu}. \end{aligned}$$

Here, the feasible set,

$$(D.4) \quad \{\mathbf{c} \mid \mathbf{X}_{\text{ms}} \mathbf{c} = \mathbf{z}_{n+1} - \boldsymbol{\mu}\},$$

is an affine subspace, which is an object that results from the set addition of a subspace and a constant vector called the offset. In representing an affine subspace, we can use any of its elements as the offset. Since [\(3.9\)](#) and [\(3.10\)](#) taken together tell us that $-\mathbf{1}_n$ is an element of [\(D.4\)](#), the latter may be rewritten as follows:

$$\{\mathbf{c} \mid \exists \mathbf{d} \in \mathcal{N}(\mathbf{X}_{\text{ms}}) \text{ such that } \mathbf{c} = -\mathbf{1}_n + \mathbf{d}\}.$$

We will now show that the closest point in this affine subspace to the origin is $-\mathcal{P}_{\mathcal{R}(\mathbf{X}_{\text{ms}}^H)}(\mathbf{1}_n)$. Consider applying [\(D.2\)](#) to $-\mathbf{1}_n$:

$$(D.5) \quad -\mathbf{1}_n = \mathcal{P}_{\mathcal{N}(\mathbf{X}_{\text{ms}})}(-\mathbf{1}_n) + \mathcal{P}_{\mathcal{R}(\mathbf{X}_{\text{ms}}^H)}(-\mathbf{1}_n)$$

If we construct

$$\tilde{\mathbf{d}} := \mathcal{P}_{\mathcal{N}(\mathbf{X}_{\text{ms}})}(-\mathbf{1}_n) + \mathbf{d},$$

then, \mathbf{c} can be re-written thus:

$$\mathbf{c} = \underbrace{-\mathbf{1}_n}_{\in \mathcal{R}(\mathbf{X}_{\text{ms}}^H)} + \mathbf{d} = \mathcal{P}_{\mathcal{R}(\mathbf{X}_{\text{ms}}^H)}(-\mathbf{1}_n) + \underbrace{\mathcal{P}_{\mathcal{N}(\mathbf{X}_{\text{ms}})}(-\mathbf{1}_n) + \mathbf{d}}_{\in \mathcal{N}(\mathbf{X}_{\text{ms}})} = \mathcal{P}_{\mathcal{R}(\mathbf{X}_{\text{ms}}^H)}(-\mathbf{1}_n) + \tilde{\mathbf{d}}.$$

Now, $\mathbf{d} \in \mathcal{N}(\mathbf{X}_{\text{ms}})$ ensures that $\tilde{\mathbf{d}}$ is also in the kernel of \mathbf{X}_{ms} . Hence, by invoking the orthogonality of $\mathcal{N}(\mathbf{X}_{\text{ms}})$ and $\mathcal{R}(\mathbf{X}_{\text{ms}}^H)$, we get:

$$\|\mathbf{c}\|^2 = \|\mathcal{P}_{\mathcal{R}(\mathbf{X}_{\text{ms}}^H)}(-\mathbf{1}_n)\|^2 + \|\tilde{\mathbf{d}}\|^2 \geq \|\mathcal{P}_{\mathcal{R}(\mathbf{X}_{\text{ms}}^H)}(-\mathbf{1}_n)\|^2.$$

So, every point in [\(D.4\)](#) has a norm of at-least $\|\mathcal{P}_{\mathcal{R}(\mathbf{X}_{\text{ms}}^H)}(-\mathbf{1}_n)\|$. Using [\(D.5\)](#), we can show that $\mathcal{P}_{\mathcal{R}(\mathbf{X}_{\text{ms}}^H)}(-\mathbf{1}_n)$ does belong to the affine subspace [\(D.4\)](#). Consequently, it is also the closest point in [\(D.4\)](#) to the origin. Thus, by [\(D.3\)](#), we find that [\(D.1\)](#) is true.

Using [\(D.2\)](#), we can now simultaneously obtain the forward and backward implications:

$$\mathbf{c}^*[\mathbf{Z}_{\text{ms}}] = -\mathbf{1}_n \implies \mathcal{P}_{\mathcal{N}(\mathbf{X}_{\text{ms}})}\mathbf{1}_n = 0 \implies \mathbf{c}^*[\mathbf{Z}_{\text{ms}}] = -\mathbf{1}_n. \quad \square$$

Note that this characterization of DMD-DFT equivalence does not invoke the existence of a finite dimensional Koopman invariant subspace.

D.2. Equivalence when \mathbf{X}_{ms} has linearly dependent columns. In order to prove [Theorem 4.2](#), we establish the following algebraic result:

LEMMA D.2.

$$\mathbf{1}_r - \left(\frac{1}{n+1}\right) \boldsymbol{\Theta} \mathbf{1}_{n+1} = -\left(\frac{1}{n+1}\right) (\Lambda - \mathbf{I}) \boldsymbol{\Theta} \mathbf{1} \begin{bmatrix} n \\ n-1 \\ \vdots \\ 1 \end{bmatrix}.$$

Proof. Consider the i -th component of the vector on the left:

$$1 - \left(\frac{1}{n+1} \right) [1 \quad \lambda_i \quad \lambda_i^2 \quad \dots \quad \lambda_i^n] \mathbf{1}_{n+1}.$$

Expanding the inner product and factoring out the denominator, we get:

$$\frac{1}{n+1} ((n+1) - (1 + \lambda_i + \lambda_i^2 + \dots + \lambda_i^n)).$$

The two sums in the numerator have $(n+1)$ terms each. By summing them in pairs, we obtain:

$$-\frac{1}{n+1} ((\lambda_i - 1) + (\lambda_i^2 - 1) + \dots + (\lambda_i^n - 1)).$$

By factoring out $(\lambda_i - 1)$ from each of the remaining n terms, we get the following:

$$-\frac{\lambda_i - 1}{n+1} [1 \quad \lambda_i \quad \dots \quad \lambda_i^{n-1}] \begin{bmatrix} n \\ n-1 \\ \vdots \\ 1 \end{bmatrix}.$$

Collect the components into a column vector, and group terms to reach the desired conclusion. \square

Proof of Theorem 4.2. We will begin by explicitly constructing the dictionary alluded to, and then show that it indeed exhibits DMD-DFT equivalence despite \mathbf{X}_{ms} having linearly dependent columns.

Constructing the counter-example:

Let \mathbf{l} denote the last column of Θ_1 and \mathbf{l}^\perp be the projection of \mathbf{l} orthogonal to the span of the first $n-1$ columns of Θ_1 .

$$(D.6) \quad \mathbf{l} := \begin{bmatrix} \lambda_1^{n-1} \\ \lambda_2^{n-1} \\ \vdots \\ \lambda_r^{n-1} \end{bmatrix}, \quad \mathbf{l}^\perp := \mathcal{P}_{\mathcal{N}(\Theta_2^H)} \mathbf{l}.$$

Here, we have used (A.5) to denote the sub-matrix formed by the first $n-1$ columns of Θ as Θ_2 . Now, by Definition 3.8, we can define the dictionary, ψ , by simply specifying the matrix $\tilde{\mathbf{C}}$:

$$(D.7) \quad \tilde{\mathbf{C}}_0 := (\mathbf{l}^\perp)^H (\mathbf{\Lambda} - \mathbf{I})^{-1}, \quad \tilde{\mathbf{C}} = \tilde{\mathbf{C}}_0 \text{diag}[\phi(\mathbf{v}_1)]^{-1}.$$

Validation:

We begin with a quick sanity check that our observables are indeed non-trivial. By (B.3), $n \leq r$ ensures that $\Theta_1 \in \mathbb{C}^{r \times n}$ has full column rank. So, \mathbf{l} , the last column of Θ_1 , will not be in the span of the remaining columns. Hence, $\mathbf{l}^\perp \neq \mathbf{0}$ and our observables, represented by $\tilde{\mathbf{C}}$, are non-trivial.

Our objective is to show that \mathbf{X}_{ms} has linearly dependent columns and also satisfies $\mathcal{P}_{\mathcal{N}(\mathbf{X}_{\text{ms}})} \mathbf{1}_n = \mathbf{0}$.

Rank defectiveness of \mathbf{X}_{ms} follows directly from its shape. The identities (3.4), (3.10), and (3.12), when taken together, tell us that \mathbf{X}_{ms} is of size $m \times n$. Since $\tilde{\mathbf{C}}$ is a row vector, $m = 1$ and, hence, \mathbf{X}_{ms} is also a row vector. The condition $n \geq 2$

means \mathbf{X}_{ms} has at least 2 columns and these must be linearly dependent as it only has a single row.

We prove DMD-DFT equivalence by showing that the data matrix \mathbf{X}_{ms} satisfies a sufficient condition. To this end, we construct a banded matrix $\mathbf{B} \in \mathbb{C}^{n \times (n-1)}$ as follows:

$$\mathbf{B} := \begin{bmatrix} -1 & & & \\ 1 & \ddots & & \\ & \ddots & -1 & \\ & & & 1 \end{bmatrix}.$$

Evidently, $\mathbf{B}^H \mathbf{1}_n = \mathbf{0}$. Indeed, the columns of \mathbf{B} form a basis for the orthogonal complement of the span of $\mathbf{1}_n$.

$$\mathcal{R}(\mathbf{B}) = \mathcal{N}(\mathbf{1}_n^H).$$

If we can show that $\mathcal{R}(\mathbf{B}) = \mathcal{N}(\mathbf{X}_{\text{ms}})$, then DMD-DFT equivalence is also true:

$$\mathcal{R}(\mathbf{B}) = \mathcal{N}(\mathbf{X}_{\text{ms}}) \implies \mathcal{P}_{\mathcal{N}(\mathbf{X}_{\text{ms}})} \mathbf{1}_n = \mathcal{P}_{\mathcal{R}(\mathbf{B})} \mathbf{1}_n = \mathcal{P}_{\mathcal{N}(\mathbf{1}_n^H)} \mathbf{1}_n = \mathbf{0}.$$

So, we have an alternative approach to proving DMD-DFT equivalence.

Before proceeding further, we perform some algebraic simplifications. The specific choice of $\tilde{\mathbf{C}}$ in (D.7), when applied alongside (A.2) to (A.3), gives,

$$\mathbf{Z} = \tilde{\mathbf{C}}_0 \Theta,$$

which in turn simplifies $\boldsymbol{\mu}$ thus:

$$(D.8) \quad \boldsymbol{\mu} = \tilde{\mathbf{C}}_0 (\Theta \mathbf{1}_{n+1}) \left(\frac{1}{n+1} \right).$$

Consequently, \mathbf{Z}_{ms} and \mathbf{X}_{ms} may be factored as follows:

$$\mathbf{Z}_{\text{ms}} = [-\boldsymbol{\mu} \quad \tilde{\mathbf{C}}_0] \begin{bmatrix} \mathbf{1}_{n+1}^T \\ \Theta \end{bmatrix}, \quad \mathbf{X}_{\text{ms}} = [-\boldsymbol{\mu} \quad \tilde{\mathbf{C}}_0] \begin{bmatrix} \mathbf{1}_n^T \\ \Theta_1 \end{bmatrix}.$$

We will first show that $\mathcal{R}(\mathbf{B}) \subseteq \mathcal{N}(\mathbf{X}_{\text{ms}})$. Consider the product $\mathbf{X}_{\text{ms}} \mathbf{B}$ in light of the columns of \mathbf{B} being orthogonal to $\mathbf{1}_n$.

$$\mathbf{X}_{\text{ms}} \mathbf{B} = [-\boldsymbol{\mu} \quad \tilde{\mathbf{C}}_0] \begin{bmatrix} \mathbf{1}_n^T \\ \Theta_1 \end{bmatrix} \mathbf{B} = \tilde{\mathbf{C}}_0 \Theta_1 \mathbf{B}.$$

The matrix product $\Theta_1 \mathbf{B}$ may be re-written as follows with a Vandermonde matrix to the right.

$$\begin{aligned} \Theta_1 \mathbf{B} &= \begin{bmatrix} \lambda_1 - 1 & \lambda_1^2 - \lambda_1 & \dots & \lambda_1^{n-1} - \lambda_1^{n-2} \\ \lambda_2 - 1 & \lambda_2^2 - \lambda_2 & \dots & \lambda_2^{n-1} - \lambda_2^{n-2} \\ \vdots & \vdots & \ddots & \vdots \\ \lambda_r - 1 & \lambda_r^2 - \lambda_r & \dots & \lambda_r^{n-1} - \lambda_r^{n-2} \end{bmatrix} \\ &= \begin{bmatrix} \lambda_1 - 1 & & & \\ & \lambda_2 - 1 & & \\ & & \ddots & \\ & & & \lambda_r - 1 \end{bmatrix} \begin{bmatrix} 1 & \lambda_1 & \dots & \lambda_1^{n-2} \\ 1 & \lambda_2 & \dots & \lambda_2^{n-2} \\ \vdots & \vdots & \ddots & \vdots \\ 1 & \lambda_r & \dots & \lambda_r^{n-2} \end{bmatrix} \\ &= (\mathbf{\Lambda} - \mathbf{I}) \Theta_2. \end{aligned}$$

This lets us use (D.7) to bring in $\mathbf{1}^\perp$, whose definition in (D.6) completes this line of thought:

$$\tilde{\mathbf{C}}_0 \underbrace{\Theta_1 \mathbf{B}} = \underbrace{\tilde{\mathbf{C}}_0(\Lambda - \mathbf{I})} \Theta_2 = \underbrace{(\mathbf{1}^\perp)^H} \Theta_2 = \mathbf{0} \implies \mathcal{R}(\mathbf{B}) \subseteq \mathcal{N}(\mathbf{X}_{\text{ms}}).$$

Now, $\mathcal{R}(\mathbf{B})$ is a $n - 1$ dimensional subspace of \mathbb{C}^n . So, if $\mathcal{R}(\mathbf{B})$ is a strict subset of $\mathcal{N}(\mathbf{X}_{\text{ms}})$, then, by the rank-nullity theorem, $\mathbf{X}_{\text{ms}} = \mathbf{0}$. Therefore, proving that $\mathbf{X}_{\text{ms}} \neq \mathbf{0}$ is enough to show that $\mathcal{R}(\mathbf{B}) = \mathcal{N}(\mathbf{X}_{\text{ms}})$. We examine the first column of \mathbf{X}_{ms} :

$$\mathbf{X}_{\text{ms}} \mathbf{e}_1 = [-\boldsymbol{\mu} \quad \tilde{\mathbf{C}}_0] \begin{bmatrix} \mathbf{1}_n^T \\ \Theta_1 \end{bmatrix} \mathbf{e}_1 = -\boldsymbol{\mu} + \tilde{\mathbf{C}}_0 \mathbf{1}_r.$$

If we expand $\boldsymbol{\mu}$ as in (D.8), it becomes amenable to apply Lemma D.2:

$$\begin{aligned} -\underbrace{\boldsymbol{\mu}} + \tilde{\mathbf{C}}_0 \mathbf{1}_r &= \tilde{\mathbf{C}}_0 \left[\mathbf{1}_r - (\Theta \mathbf{1}_{n+1}) \left(\frac{1}{n+1} \right) \right] \\ &= \tilde{\mathbf{C}}_0 (\Lambda - \mathbf{I}) \Theta_1 \begin{bmatrix} n \\ n-1 \\ \vdots \\ 1 \end{bmatrix} \left(\frac{-1}{n+1} \right). \end{aligned}$$

Once again, we can use (D.6) and (D.7) to introduce $\mathbf{1}^\perp$ and leverage its orthogonality to the first $n - 1$ columns of Θ_1 :

$$\begin{aligned} \underbrace{\tilde{\mathbf{C}}_0(\Lambda - \mathbf{I})} \Theta_1 \begin{bmatrix} n \\ n-1 \\ \vdots \\ 1 \end{bmatrix} \left(\frac{-1}{n+1} \right) &= \underbrace{(\mathbf{1}^\perp)^H \Theta_1} \begin{bmatrix} n \\ n-1 \\ \vdots \\ 1 \end{bmatrix} \left(\frac{-1}{n+1} \right) \\ &= \underbrace{(\mathbf{1}^\perp)^H \mathbf{1}} \left(\frac{-1}{n+1} \right) \\ &= \|\mathbf{1}^\perp\|^2 \left(\frac{-1}{n+1} \right). \end{aligned}$$

Since we've already seen that $\mathbf{1}^\perp \neq \mathbf{0}$, the matrix-vector product $\mathbf{X}_{\text{ms}} \mathbf{e}_1 \neq \mathbf{0}$ and, consequently, we have DMD-DFT equivalence. \square

D.3. A modal decomposition of mean-subtracted data. When the Koopman mode expansion possesses only a finite number of terms, Lemma A.1 tells us that the time series \mathbf{Z} can be written as the product of \mathbf{C} and Θ . Here, we derive an analogous factorization for the mean-removed data-set \mathbf{Z}_{ms} .

DEFINITION D.3 (A conformal partitioning of \mathbf{C} and Θ). *Suppose (3.8) and (3.10) are true. Additionally, let 1 be a Koopman eigenvalue i.e., $1 \in \{\lambda_i\}_{i=1}^r$. Then, (A.3) motivates defining \mathbf{c}_1 , $\mathbf{C}_{\neq 1}$ and $\Theta_{\neq 1}$ via the following conformal partitioning:*

$$(D.9) \quad \mathbf{C} =: [\mathbf{c}_1 \quad \mathbf{C}_{\neq 1}], \quad \Theta =: \begin{bmatrix} \mathbf{1}_{n+1}^T \\ \Theta_{\neq 1} \end{bmatrix}.$$

To paraphrase, \mathbf{c}_1 is the column of \mathbf{C} that multiplies $\mathbf{1}_{n+1}^T$ in the product $\mathbf{C}\Theta$, $\mathbf{C}_{\neq 1}$ is the sub-matrix of \mathbf{C} obtained by excluding \mathbf{c}_1 and $\Theta_{\neq 1}$ is the sub-matrix of Θ produced by deleting the row corresponding to $\mathbf{1}_{n+1}^T$.

TABLE D.1

Constructing \mathbf{C}_{ms} and Θ_{ms} : There are four possible scenarios in mean-subtraction, depending on the presence of a Koopman eigenvalue at 1 (Branch 1) and the value of $\boldsymbol{\mu}$ (Branch 2). The peculiarities of each case are incorporated in the definitions of \mathbf{C}_{ms} and Θ_{ms} (last two columns), with an eye towards inducing an analogue of (A.3) for \mathbf{Z}_{ms} .

Case	Branch 1	Branch 2	\mathbf{C}_{ms}	Θ_{ms}
I	$1 \notin \{\lambda_i\}_{i=1}^r$	$\boldsymbol{\mu} = \mathbf{0}$	\mathbf{C}	Θ
II	"	$\boldsymbol{\mu} \neq \mathbf{0}$	$[\mathbf{C} \quad -\boldsymbol{\mu}]$	$\begin{bmatrix} \Theta \\ \mathbf{1}_{n+1}^T \end{bmatrix}$
III	$1 \in \{\lambda_i\}_{i=1}^r$	$\boldsymbol{\mu} = \mathbf{c}_1$	$\mathbf{C}_{\neq 1}$	$\Theta_{\neq 1}$
IV	"	$\boldsymbol{\mu} \neq \mathbf{c}_1$	$[\mathbf{c}_1 - \boldsymbol{\mu} \quad \mathbf{C}_{\neq 1}]$	$\begin{bmatrix} \mathbf{1}_{n+1}^T \\ \Theta_{\neq 1} \end{bmatrix}$

LEMMA D.4. Suppose (3.8) and (3.10) are true. If we construct the two matrices \mathbf{C}_{ms} and Θ_{ms} as described by Definition D.3 and Table D.1, then, every column of \mathbf{C}_{ms} is non-zero, Θ_{ms} has distinct nodes and, more importantly,

$$(D.10) \quad \mathbf{Z}_{\text{ms}} = \mathbf{C}_{\text{ms}} \Theta_{\text{ms}}.$$

In other words, every row of \mathbf{Z}_{ms} lies in the row space of the Vandermonde matrix Θ_{ms} , which is related to but potentially different from Θ .

Proof. A direct application of Lemma A.1 to (3.10), in the context of Definition D.3 and Table D.1. \square

Remark D.5. We can extend the parallel between (A.3) and (D.10) by defining $(\Theta_{\text{ms}})_j$ to be the sub-matrix of Θ_{ms} produced by deleting the last j columns. Consequently, \mathbf{X}_{ms} (defined in (3.12)) has the following Koopman mode factorization:

$$(D.11) \quad \mathbf{X}_{\text{ms}} = \mathbf{C}_{\text{ms}} (\Theta_{\text{ms}})_1.$$

Remark D.6. The analogy between (A.3) and (D.10) suggests that the nodes of Θ_{ms} will be as central to the upcoming analysis, as the nodes of Θ (namely the Koopman eigenvalues $\{\lambda_i\}_{i=1}^r$) were in the justification of Theorem 3.4. Hence, we formally recognize them thus:

$$\sigma(\Theta_{\text{ms}}) := \text{Nodes of the Vandermonde matrix } \Theta_{\text{ms}}.$$

D.4. Over-sampling and linear consistency prevent equivalence. We preface the justification of Theorem 4.3 by partitioning the outcome of mean subtraction into four scenarios, depending on the presence of 1 in the ‘‘mean-subtracted Koopman spectrum’’ $\sigma(\Theta_{\text{ms}})$ and the Koopman spectrum $\{\lambda_i\}_{i=1}^r$ (Table D.2). This classification helps develop auxiliary guarantees on the temporal mean and \mathbf{C}_{ms} which simplify the proof of Theorem 4.3.

Firstly, we show that a Koopman invariant dictionary ensures a non-zero mean $\boldsymbol{\mu}$, except in Case III. This is proven in three parts and begins by studying Cases II and IV:

PROPOSITION D.7. Suppose (3.8) and (3.10) are true. If $\tilde{\mathbf{C}}$ has full column rank and 1 is a Koopman eigenvalue i.e., $1 \in \{\lambda_i\}_{i=1}^r$, then, the temporal mean $\boldsymbol{\mu} \neq \mathbf{0}$.

TABLE D.2

Delineating the effect of mean subtraction: There are four possible outcomes of mean-removal, depending on the presence (or absence) of 1 in the nodes of Θ_{ms} (Branch 1) and in the Koopman eigen-values (Branch 2). For each case, we detail $\sigma(\Theta_{\text{ms}})$ alongside \mathbf{C}_{ms} and Θ_{ms} (whenever they have a simple expression).

Case	Branch 1	Branch 2	$\sigma(\Theta_{\text{ms}})$	\mathbf{C}_{ms}	Θ_{ms}
I	$1 \in \sigma(\Theta_{\text{ms}})$	$1 \notin \{\lambda_i\}_{i=1}^r$	$\{\lambda_i\}_{i=1}^r \cup \{1\}$		
II	"	$1 \in \{\lambda_i\}_{i=1}^r$	$\{\lambda_i\}_{i=1}^r$		Θ
III	$1 \notin \sigma(\Theta_{\text{ms}})$	$1 \notin \{\lambda_i\}_{i=1}^r$	$\{\lambda_i\}_{i=1}^r$	\mathbf{C}	Θ
IV	"	$1 \in \{\lambda_i\}_{i=1}^r$	$\{\lambda_i\}_{i=1}^r \cap \{1\}^c$	$\mathbf{C}_{\neq 1}$	

Proof. When (3.8) is true, the time-average $\boldsymbol{\mu}$, which is defined in (3.9), can be expanded using (A.3) as follows:

$$\boldsymbol{\mu} = \frac{1}{n+1} \mathbf{C} \Theta \mathbf{1}_{n+1}.$$

Now, $1 \in \{\lambda_i\}_{i=1}^r$ ensures that $\Theta \mathbf{1}_{n+1}$ has at least one non-zero coefficient and, hence, is non-zero. Furthermore, (3.10) lets the full column rank of $\tilde{\mathbf{C}}$ be inherited by \mathbf{C} . Combining these two inferences, we get $\boldsymbol{\mu} \neq \mathbf{0}$. \square

Case I is tackled by finding a necessary condition for zero mean and taking the contrapositive.

PROPOSITION D.8. *Suppose (3.8) and (3.10) are true. If the temporal mean $\boldsymbol{\mu} = \mathbf{0}$ and $1 \in \sigma(\Theta_{\text{ms}})$, then $\tilde{\mathbf{C}}$ has linearly dependent columns.*

Proof. By (3.10), it is sufficient to establish that the vector,

$$\mathbf{z} := \Theta \mathbf{1}_{n+1},$$

is a non-trivial element of $\mathcal{N}(\mathbf{C})$.

Firstly, by the definitions of \mathbf{C}_{ms} and Θ_{ms} in Table D.1, we have,

$$\boldsymbol{\mu} = \mathbf{0} \implies \mathbf{C}_{\text{ms}} = \mathbf{C}, \Theta_{\text{ms}} = \Theta.$$

As a result, the condition $1 \in \sigma(\Theta_{\text{ms}})$ translates, by (A.1), to $1 \in \{\lambda_i\}_{i=1}^r$, which once again gives $\Theta \mathbf{1}_{n+1} = \mathbf{z} \neq \mathbf{0}$. Consequently, unpacking the action of \mathbf{C} on \mathbf{z} yields the desired conclusion:

$$\mathbf{C} \underbrace{\mathbf{z}}_{\frac{1}{n+1}} = \underbrace{\mathbf{C} \Theta \mathbf{1}_{n+1}}_{\frac{1}{n+1}} = \boldsymbol{\mu} = \mathbf{0} \implies \mathbf{z} \in \mathcal{N}(\mathbf{C}). \quad \square$$

Compiling the above results and studying Case III, we find that it is the only scenario when the mean is $\mathbf{0}$.

LEMMA D.9. *Suppose (3.8) and (3.10) are true. If $\tilde{\mathbf{C}}$ has full column rank, then, the mean $\boldsymbol{\mu}$ is zero only in Case III of Table D.2.*

$$\boldsymbol{\mu} = \mathbf{0} \iff \text{Case III.}$$

Proof. We prove the forward implication by contraposition. Consider Cases I, II and IV in Table D.2. By Proposition D.7, the mean is non-zero for Cases II and IV. In Case I, we have $1 \in \sigma(\Theta_{\text{ms}})$. Since $\tilde{\mathbf{C}}$ has linearly independent columns, we can apply the contrapositive of Proposition D.8 to show $\boldsymbol{\mu} \neq \mathbf{0}$.

The backward implication is proven by contradiction. Suppose we have Case III and $\boldsymbol{\mu} \neq \mathbf{0}$. Since $1 \notin \{\lambda_i\}_{i=1}^r$, removing the non-zero mean from \mathbf{Z} will simply cause $1 \in \sigma(\boldsymbol{\Theta}_{\text{ms}})$ which is in contradiction with Case III. \square

Now, we proceed to connect the range of \mathbf{C}_{ms} to those of \mathbf{C} and $\mathbf{C}_{\neq 1}$. The definition of \mathbf{C}_{ms} in (D.10) belies the intricacies of mean subtraction that are detailed in Table D.2. Starting with the matrix \mathbf{C} , it is possible to gain (Case I) or lose (Case IV) a column. An existing column may be modified (Case II) or there may no effect whatsoever (Case III). Fortunately, we need only understand the relationship between the column spaces of \mathbf{C}_{ms} , \mathbf{C} and their sub-matrices.

PROPOSITION D.10. *Suppose (3.8) and (3.10) are true. Then,*

$$\begin{aligned}\boldsymbol{\mu} = \mathbf{0} &\implies \mathbf{C}_{\text{ms}} = \mathbf{C}. \\ \boldsymbol{\mu} \neq \mathbf{0} &\implies \mathcal{R}(\mathbf{C}_{\text{ms}}) = \mathcal{R}(\mathbf{C}_{\neq 1}).\end{aligned}$$

Additionally, if we define $(\mathbf{C}_{\text{ms}})_{\neq 1}$ to be the analogue of $\mathbf{C}_{\neq 1}$ for \mathbf{C}_{ms} ¹⁹, we also get:

$$\mathcal{R}((\mathbf{C}_{\text{ms}})_{\neq 1}) = \mathcal{R}(\mathbf{C}_{\neq 1}).$$

Proof. Follows from the definitions of \mathbf{C} (A.2) and \mathbf{C}_{ms} (Table D.1), with routine algebraic manipulations. \square

Technically, we are now embarking on the proof of Theorem 4.3. However, the arguments involved are also useful in establishing Corollary 4.5. So, they have been organized into the two theorems below to facilitate their reuse. Both of these are proven by contradiction and we begin by studying Cases III and IV.

THEOREM D.11. *Suppose (3.8) and (3.10) are true. Additionally, assume that $1 \notin \sigma(\boldsymbol{\Theta}_{\text{ms}})$. If the training data is well-sampled i.e., $n \geq r$, then mean-subtracted DMD is not DFT for Case IV in Table D.2. Under the stronger condition of over-sampling ($n \geq r + 1$), non-equivalence holds for Case III too.*

Proof. We prove both cases by contradiction. Suppose mean-subtracted DMD is equivalent to DFT, as detailed in Definition 3.7. Then, by Theorem 4.1, we have:

$$\mathcal{P}_{\mathcal{N}(\mathbf{X}_{\text{ms}})} \mathbf{1}_n = \mathbf{0}.$$

Since $\mathcal{N}(\mathbf{X}_{\text{ms}})^\perp = \mathcal{R}(\mathbf{X}_{\text{ms}}^H)$, an equivalent statement would be:

$$\exists \mathbf{d} \text{ such that } \mathbf{d}^H \mathbf{X}_{\text{ms}} = \mathbf{1}_n^H.$$

Shifting $\mathbf{1}_n^H$ to the left and using (D.11), we obtain an equivalent statement:

$$\exists \mathbf{d} \text{ such that } [\mathbf{d}^H \mathbf{C}_{\text{ms}} \quad -1] \begin{bmatrix} (\boldsymbol{\Theta}_{\text{ms}})_1 \\ \mathbf{1}_n^H \end{bmatrix} = \mathbf{0}.$$

Hence, $\boldsymbol{\Theta}_{\text{aug}} := \begin{bmatrix} (\boldsymbol{\Theta}_{\text{ms}})_1 \\ \mathbf{1}_n^H \end{bmatrix}$ has linearly dependent rows.

But, the lower bounds on n mean that $\boldsymbol{\Theta}_{\text{aug}}$ has full row rank. Firstly, $1 \notin \sigma(\boldsymbol{\Theta}_{\text{ms}})$ ensures that $\boldsymbol{\Theta}_{\text{aug}}$ has distinct nodes. While it has n columns, the number of rows is case dependent. In Case III, $\boldsymbol{\Theta}_{\text{aug}}$ has $r+1$ rows and at least $r+1$ columns. Similarly, in Case IV, $\boldsymbol{\Theta}_{\text{aug}}$ has r rows and at least r columns. Hence, in both cases, (B.2) tells us that $\boldsymbol{\Theta}_{\text{aug}}$ has full row rank which is a contradiction. \square

¹⁹Specifically, $(\mathbf{C}_{\text{ms}})_{\neq 1}$ is taken to be the sub-matrix of \mathbf{C}_{ms} formed by excluding the column (if it exists) corresponding to the eigenvalue at 1

Cases I and II have a similar proof strategy where [Proposition D.10](#) plays a crucial role.

THEOREM D.12. *Suppose (3.8) and (3.10) are true. Additionally, assume that we have $1 \in \sigma(\Theta_{\text{ms}})$ and a full column rank $\tilde{\mathbf{C}}$. If $n \geq r$, then mean-subtracted DMD is not DFT for Case II in [Table D.2](#). If $n \geq r + 1$, non-equivalence also holds for Case I.*

Proof. As with [Theorem D.11](#), we prove by contradiction. Assuming we have DMD-DFT equivalence, we can sequentially apply [Theorem 4.1](#) and the identity, $\mathcal{N}(\mathbf{X}_{\text{ms}})^\perp = \mathcal{R}(\mathbf{X}_{\text{ms}}^H)$, to get the following assertion:

$$\exists \mathbf{d} \text{ such that } \mathbf{d}^H \mathbf{X}_{\text{ms}} = \mathbf{1}_n^H.$$

Using [\(D.11\)](#), we then get:

$$(D.12) \quad \exists \mathbf{d} \text{ such that } (\mathbf{d}^H \mathbf{C}_{\text{ms}})(\Theta_{\text{ms}})_1 = \mathbf{1}_n^H.$$

Observe that the bounds on n endow $(\Theta_{\text{ms}})_1$ with linearly independent rows. In Case I, $(\Theta_{\text{ms}})_1 \in \mathbb{C}^{(r+1) \times n}$ and $n \geq r + 1$. Case II has $(\Theta_{\text{ms}})_1 \in \mathbb{C}^{r \times n}$ and $n \geq r$. Therefore, [\(B.2\)](#) says $(\Theta_{\text{ms}})_1$ has full row rank.

Consequently, $\mathbf{d}^H \mathbf{C}_{\text{ms}}$ is the unique representation of $\mathbf{1}_n^H$ in the row space of $(\Theta_{\text{ms}})_1$. Additionally, $1 \in \sigma(\Theta_{\text{ms}})$ i.e., 1 is a node of $(\Theta_{\text{ms}})_1$. So, $\mathbf{d}^H \mathbf{C}_{\text{ms}}$ must be zero at all indices except that corresponding to the node at 1. Hence,

$$\mathbf{d}^H (\mathbf{C}_{\text{ms}})_{\neq 1} = \mathbf{0}.$$

Now, [Proposition D.10](#) says $\mathcal{R}((\mathbf{C}_{\text{ms}})_{\neq 1}) = \mathcal{R}(\mathbf{C}_{\neq 1})$. This gives:

$$\mathbf{d}^H \mathbf{C}_{\neq 1} = \mathbf{0}.$$

Since we are not dealing with Case III, [Lemma D.9](#) gives $\boldsymbol{\mu} \neq \mathbf{0}$. So, [Proposition D.10](#) also says that $\mathcal{R}(\mathbf{C}_{\text{ms}}) = \mathcal{R}(\mathbf{C}_{\neq 1})$. Thus, we get,

$$\mathbf{d}^H \mathbf{C}_{\text{ms}} = \mathbf{0},$$

which contradicts [\(D.12\)](#). □

Putting together the above results gives a deceptively short proof for the non-equivalence of mean-subtracted DMD and DFT in the over-sampled regime.

Proof of [Theorem 4.3](#). We can preface the justification by observing that the conditions of [Proposition C.2](#) are met, thereby endowing the matrix $\tilde{\mathbf{C}}$ with linearly independent columns.

The proof consists of two branches:

1. $1 \in \sigma(\Theta_{\text{ms}})$: Since all the conditions for [Theorem D.12](#) are met, there is no DMD-DFT equivalence.
2. $1 \notin \sigma(\Theta_{\text{ms}})$: Since $n \geq r + 1$, by [Theorem D.11](#), there is no DMD-DFT equivalence. □

D.5. Exploring the under and just-sampled regimes. [Lemma 3.6](#) explains the under-sampled regime. Alas, the just-sampled scenario does not afford such a simple explanation. To substantiate this, we begin by formalizing an intermediary of import.

PROPOSITION D.13. *Suppose (3.8) and (3.10) are true. If the columns of $\tilde{\mathbf{C}}$ are linearly independent and 1 is a node of Θ_{ms} , then, $\mathcal{N}(\mathbf{C}_{\text{ms}})$ is the one-dimensional subspace spanned by $\Theta_{\text{ms}}\mathbf{1}_{n+1}$.*

$$\tilde{\mathbf{C}} \text{ has full column rank \& } 1 \in \sigma(\Theta_{\text{ms}}) \implies \mathcal{N}(\mathbf{C}_{\text{ms}}) = \mathcal{R}(\Theta_{\text{ms}}\mathbf{1}_{n+1}).$$

Proof. We begin by showing that $\mathcal{N}(\mathbf{C}_{\text{ms}})$ contains $\mathcal{R}(\Theta_{\text{ms}}\mathbf{1}_{n+1})$. Consider \mathbf{Z}_{ms} as defined in (3.10). Computing the average of its columns and applying (3.9) gives:

$$\mathbf{Z}_{\text{ms}} \frac{\mathbf{1}_{n+1}}{n+1} = \mathbf{0}.$$

Expanding \mathbf{Z}_{ms} using (D.10) and invoking the definition of $\mathcal{N}(\mathbf{C}_{\text{ms}})$, we find

$$\underbrace{\mathbf{Z}_{\text{ms}}}_{n+1} \frac{\mathbf{1}_{n+1}}{n+1} = \mathbf{0} \iff \mathbf{C}_{\text{ms}} \underbrace{\Theta_{\text{ms}}\mathbf{1}_{n+1}} = \underbrace{\mathbf{0}} \implies \mathcal{N}(\mathbf{C}_{\text{ms}}) \supseteq \mathcal{R}(\Theta_{\text{ms}}\mathbf{1}_{n+1}).$$

We will show that the set containment proceeds both ways, and the condition $1 \in \sigma(\Theta_{\text{ms}})$ helps simplify this process.

Firstly, $1 \in \sigma(\Theta_{\text{ms}})$ means $\Theta_{\text{ms}}\mathbf{1}_{n+1} \neq \mathbf{0}$. Therefore, $\mathcal{R}(\Theta_{\text{ms}}\mathbf{1}_{n+1})$ is a non-trivial subspace of dimension 1. Secondly, by the contrapositive of Proposition D.8, 1 being a node of Θ_{ms} ensures that $\boldsymbol{\mu} \neq \mathbf{0}$. Consequently, we can apply Proposition D.10 to get $\mathcal{R}(\mathbf{C}_{\text{ms}}) = \mathcal{R}(\mathbf{C}_{\neq 1})$. By the rank-nullity theorem, we then obtain:

$$\dim(\mathcal{N}(\mathbf{C}_{\text{ms}})) = \text{Number of columns in } \mathbf{C}_{\text{ms}} - \dim(\mathcal{R}(\mathbf{C}_{\neq 1})).$$

Table D.2 gives us the inputs needed to compute $\dim(\mathcal{N}(\mathbf{C}_{\text{ms}}))$, and the analysis splits into two branches:

1. $1 \notin \{\lambda_i\}_{i=1}^r$ (Case I): The Vandermonde matrix Θ_{ms} has $r+1$ rows. So, by (D.10), \mathbf{C}_{ms} has $r+1$ columns. Since $1 \notin \{\lambda_i\}_{i=1}^r$, $\mathbf{C}_{\neq 1}$ coincides with \mathbf{C} which, by (3.10), inherits from $\tilde{\mathbf{C}}$ a full column rank of r . Hence,

$$\dim(\mathcal{N}(\mathbf{C}_{\text{ms}})) = (r+1) - (r) = 1.$$

2. $1 \in \{\lambda_i\}_{i=1}^r$ (Case II): The matrix \mathbf{C}_{ms} has r columns as Θ_{ms} has r rows. Since $1 \in \{\lambda_i\}_{i=1}^r$ and $\tilde{\mathbf{C}}$ has full column rank, (3.10) says that $\mathbf{C}_{\neq 1}$ has $r-1$ linearly independent columns. Therefore, we have:

$$\dim(\mathcal{N}(\mathbf{C}_{\text{ms}})) = (r) - (r-1) = 1.$$

Since we already know that this null space contains the span of $\Theta_{\text{ms}}\mathbf{1}_{n+1}$, we get:

$$\mathcal{N}(\mathbf{C}_{\text{ms}}) = \mathcal{R}(\Theta_{\text{ms}}\mathbf{1}_{n+1}). \quad \square$$

Corollary 4.5 is now amenable to reasoning:

Proof of Corollary 4.5. There are two distinct segments to this proof, corresponding to the under-sampled ($n < r$) and the just-sampled ($n = r$) regimes. We preface the discussion by highlighting a consequence of Proposition A.3 - the matrices $\tilde{\mathbf{C}}$ and \mathbf{C} both have full column rank.

- $n < r$: The analysis of this regime splits according to ‘‘Branch 1’’ in Table D.2. The primary focus will be to show that \mathbf{X}_{ms} has full column rank. DMD-DFT equivalence follows as a consequence of Lemma 3.6.

1. $1 \notin \sigma(\Theta_{\text{ms}})$ (Cases III, IV): The matrix \mathbf{C}_{ms} is either \mathbf{C} or $\mathbf{C}_{\neq 1}$, both of which have full column rank. So, $(\Theta_{\text{ms}})_1$ has at least $r - 1$ rows. Since it has n columns, for $n \leq r - 1$, it will have full column rank according to (B.3). Therefore, $\mathbf{X}_{\text{ms}} = \mathbf{C}_{\text{ms}}(\Theta_{\text{ms}})_1$ will have linearly independent columns.
2. $1 \in \sigma(\Theta_{\text{ms}})$ (Cases I, II): To prove by contradiction, suppose

$$\exists \mathbf{z} \neq \mathbf{0} \text{ such that } \mathbf{X}_{\text{ms}}\mathbf{z} = \mathbf{0}.$$

According to (D.11), we can expand \mathbf{X}_{ms} to get:

$$\exists \mathbf{z} \neq \mathbf{0} \text{ such that } \mathbf{C}_{\text{ms}}(\Theta_{\text{ms}})_1\mathbf{z} = \mathbf{0}.$$

By Proposition D.13, we know $\mathcal{N}(\mathbf{C}_{\text{ms}}) = \mathcal{R}(\Theta_{\text{ms}}\mathbf{1}_{n+1})$. Hence, there exists a scalar β such that:

$$(\Theta_{\text{ms}})_1\mathbf{z} = \beta\Theta_{\text{ms}}\mathbf{1}_{n+1} \iff \Theta_{\text{ms}} \begin{bmatrix} \mathbf{z} - \beta\mathbf{1}_n \\ -\beta \end{bmatrix} = \mathbf{0}.$$

Table D.2 says Θ_{ms} has $n+1$ columns and at least r rows. Since $n+1 \leq r$, (B.3) says Θ_{ms} has full column rank. Using this in the above expression, we have $\beta = 0$ and $\mathbf{z} = \mathbf{0}$, which contradicts our assumption that $\mathbf{z} \neq \mathbf{0}$. Hence, \mathbf{X}_{ms} has full column rank.

- $n = r$: Just-sampling necessitates a case-by-case handling of the scenarios described in Table D.2.
 1. Case I: The arguments are very similar to the proof for $n < r$. Suppose there exists $\mathbf{z} \neq \mathbf{0}$ satisfying $\mathbf{X}_{\text{ms}}\mathbf{z} = \mathbf{0}$. Once again, Proposition D.13, taken together with (D.11), says there exists β such that

$$\Theta_{\text{ms}} \begin{bmatrix} \mathbf{z} - \beta\mathbf{1}_n \\ -\beta \end{bmatrix} = \mathbf{0}.$$

In Case I, Θ_{ms} has dimensions $r+1 \times r+1$. By (B.2), we find that Θ_{ms} is invertible. Thus, $\beta = 0$ and $\mathbf{z} = \mathbf{0}$ which is a contradiction. Hence, \mathbf{X}_{ms} is full column rank which ensures DMD-DFT equivalence.

2. Case II: We have $n = r$ and $1 \in \sigma(\Theta_{\text{ms}})$ along with a full column rank $\tilde{\mathbf{C}}$. Hence, by Theorem D.12, there is no DMD-DFT equivalence.
3. Case III: According to Lemma D.9, $\boldsymbol{\mu} = \mathbf{0}$. So, by (A.7), we have $\mathbf{X}_{\text{ms}} = \mathbf{X} = \mathbf{C}\Theta_1$. Equation (B.3) tells us that the matrix $\Theta_1 \in \mathbb{C}^{r \times r}$ has full column rank. Hence, \mathbf{X}_{ms} has full column rank and, therefore, we have DMD-DFT equivalence by Lemma 3.6.
4. Case IV: The similarity of (D.10) to (A.3) lets us view the columns of \mathbf{Z}_{ms} as snapshots of the same dynamical system along the same trajectory starting at \mathbf{v}_1 , but generated using a potentially different set of observables. Here, in Case IV, the new dictionary lies in the non-redundant span of the $r - 1$ KEFs that correspond to the eigen-values $\sigma(\Theta_{\text{ms}}) = \{\lambda_i\}_{i=1}^r \cap \{1\}^c$. The initial condition \mathbf{v}_1 continues to be spectrally informative for this modified collection of observables. Furthermore, note that
 - The matrix $\mathbf{C}_{\text{ms}} = \mathbf{C}_{\neq 1}$ has full column rank. So, by Proposition A.3, the new dictionary is also Koopman invariant- a property that, by definition, guarantees the pertinent inputs to DMD are linearly consistent.

- The mean-subtracted time series \mathbf{Z}_{ms} has zero temporal mean.
- The number of columns in $\mathbf{X}_{\text{ms}}(r)$ is at least 1 more than the number of distinct KEFs ($r-1$) whose non-redundant span contains the new observables.

Applying [Theorem 4.3](#), we see that there is no DMD-DFT equivalence. \square

D.6. Delay embedding can generate a Koopman invariant dictionary.

Taking time delays is a simple and pragmatic way to produce a Koopman invariant dictionary from ψ ([Proposition 4.6](#)). To substantiate this claim, consider the matrices $\tilde{\mathbf{C}}_{\text{d-delayed}}$ and $\mathbf{C}_{\text{d-delayed}}$ defined as the delay-embedded counterparts of $\tilde{\mathbf{C}}$ and \mathbf{C} respectively.

$$(D.13) \quad \tilde{\mathbf{C}}_{\text{d-delayed}} := \begin{bmatrix} \tilde{\mathbf{C}} \\ \tilde{\mathbf{C}}\Lambda \\ \vdots \\ \tilde{\mathbf{C}}\Lambda^d \end{bmatrix}, \quad \mathbf{C}_{\text{d-delayed}} := \begin{bmatrix} \mathbf{C} \\ \mathbf{C}\Lambda \\ \vdots \\ \mathbf{C}\Lambda^d \end{bmatrix}.$$

Using the definition of Θ_d from [\(A.5\)](#) in [\(4.2\)](#), we find:

$$\mathbf{Z}_{\text{d-delayed}} = \mathbf{C}_{\text{d-delayed}} \Theta_d.$$

Moreover, [\(A.2\)](#) tells us how to connect $\mathbf{C}_{\text{d-delayed}}$ and $\tilde{\mathbf{C}}_{\text{d-delayed}}$:

$$\mathbf{C}_{\text{d-delayed}} = \tilde{\mathbf{C}}_{\text{d-delayed}} \text{diag}[\phi(\mathbf{v}_1)].$$

The preceding arguments, taken in light of the derivation in [Appendix A.1](#) that gives [\(A.3\)](#), suggest that $\tilde{\mathbf{C}}_{\text{d-delayed}}$ is the representation of $\psi_{\text{d-delayed}}$ in the eigen-basis ϕ :

$$\psi_{\text{d-delayed}} = \tilde{\mathbf{C}}_{\text{d-delayed}} \phi.$$

With this machinery in place, a classical argument from systems theory, reviewed here as [Lemma D.14](#), shows that $r-1$ delays are sufficient for $\psi_{\text{d-delayed}}$ to be Koopman invariant.

LEMMA D.14 (Eigenvector test for Observability [8]). *Let \mathbf{A} and \mathbf{C} denote two matrices belonging to $\mathbb{C}^{r \times r}$ and $\mathbb{C}^{m \times r}$ respectively. Consider their observability matrix, which is defined thus:*

$$\text{obs}(\mathbf{A}, \mathbf{C}) := \begin{bmatrix} \mathbf{C} \\ \mathbf{C}\mathbf{A} \\ \vdots \\ \mathbf{C}\mathbf{A}^{r-1} \end{bmatrix}.$$

If no eigenvector of \mathbf{A} lies in the null-space of \mathbf{C} , then, the columns of $\text{obs}(\mathbf{A}, \mathbf{C})$ are linearly independent.

$\{\mathbf{v} \neq \mathbf{0} \mid \exists \lambda \text{ such that } \mathbf{A}\mathbf{v} = \lambda\mathbf{v}\} \cap \mathcal{N}(\mathbf{C}) = \{\} \implies \text{obs}(\mathbf{A}, \mathbf{C}) \text{ has full column rank.}$

Proof of Proposition 4.6. The assumption that ψ lies in the non-redundant span of r distinct KEFs ensures, by [Definition 3.8](#), that every column of $\tilde{\mathbf{C}}$ is non-zero. Hence, by [\(D.13\)](#), we find that every column of $\tilde{\mathbf{C}}_{\text{d-delayed}}$ is also non-zero.

Consequently, we can apply [Proposition A.3](#) for $\psi_{d\text{-delayed}}$, which tells us that Koopman invariance of $\psi_{d\text{-delayed}}$ can be established by showing that the columns of $\tilde{\mathbf{C}}_{d\text{-delayed}}$ are linearly independent. This can, in turn, be proven by applying [Lemma D.14](#) for the matrix pair $(\mathbf{A}, \tilde{\mathbf{C}})$.

The eigenvectors of \mathbf{A} are the standard basis vectors. The assumption [\(3.8\)](#) guarantees that no column of $\tilde{\mathbf{C}}$ is $\mathbf{0}$. Hence, by [Lemma D.14](#), $\text{obs}(\mathbf{A}, \tilde{\mathbf{C}})$ has full column rank. Now, $d \geq r - 1$ ensures that the rows of $\text{obs}(\mathbf{A}, \tilde{\mathbf{C}})$ form a subset of the rows in $\tilde{\mathbf{C}}_{d\text{-delayed}}$. Therefore, $\tilde{\mathbf{C}}_{d\text{-delayed}}$ also has full column rank. \square

D.7. Relative distance to DFT. In $d\mu\text{DMD}$ ([Algorithm 4.1](#)), DMD-DFT equivalence is defined in terms of a set equality ([Definition 4.8](#)). Since set equalities are not numerically well-defined, we develop a computationally tractable alternative dubbed **Relative distance to DFT**. Constructing this indicator necessitates unpacking [Algorithm 4.1](#) and results in a characterization²⁰ that revolves around a vector equality.

Let $\boldsymbol{\mu}_{d\text{-delayed}}$ denote the temporal mean of $\mathbf{Z}_{d\text{-delayed}}$:

$$\boldsymbol{\mu}_{d\text{-delayed}} := \mathbf{Z}_{d\text{-delayed}} \frac{\mathbf{1}_{\theta+1}}{\theta + 1}.$$

The mean-subtracted version of $\mathbf{Z}_{d\text{-delayed}}$ would, then, read:

$$(D.14) \quad (\mathbf{Z}_{d\text{-delayed}})_{\text{ms}} := \mathbf{Z}_{d\text{-delayed}} - \boldsymbol{\mu}_{d\text{-delayed}} \mathbf{1}_{\theta+1}^T.$$

The resulting DMD model, $\mathbf{c}^*[(\mathbf{Z}_{d\text{-delayed}})_{\text{ms}}]$, encodes the $d\mu\text{DMD}$ eigen-values, $\{\check{\lambda}_i\}_{i=1}^\theta$. Since the latter is at the heart of [Definition 4.8](#) being numerically ill-defined, we use the former to get the following reformulation:

LEMMA D.15 (Recasting $d\mu\text{DMD} \equiv \text{DFT}$ as a vector equality). *A necessary and sufficient condition for $d\mu\text{DMD}$ to be equivalent²¹ to a temporal DFT is that the $d\mu\text{DMD}$ model, $\mathbf{c}^*[(\mathbf{Z}_{d\text{-delayed}})_{\text{ms}}]$, coincide with $-\mathbf{1}_\theta$:*

$$d\mu\text{DMD} \equiv \text{DFT} \iff \mathbf{c}^*[(\mathbf{Z}_{d\text{-delayed}})_{\text{ms}}] = -\mathbf{1}_\theta.$$

Proof. By [Definition 4.8](#), the left-hand side can be expanded in terms of the $d\mu\text{DMD}$ eigenvalues, $\{\check{\lambda}_i\}_{i=1}^\theta$.

$$d\mu\text{DMD} \equiv \text{DFT} \iff \{\check{\lambda}_i\}_{i=1}^\theta = \{z \neq 1 \mid z^{\theta+1} = 1\}.$$

Since $\{\check{\lambda}_i\}_{i=1}^\theta$ are defined in [Algorithm 4.1](#) to be the eigenvalues of the Companion matrix $\mathbf{T}(\mathbf{c}^*[(\mathbf{Z}_{d\text{-delayed}})_{\text{ms}}])$, we have the desired conclusion. \square

Hence, the root-mean-squared error between $\mathbf{c}^*[(\mathbf{Z}_{d\text{-delayed}})_{\text{ms}}]$ and $-\mathbf{1}_\theta$ can measure the deviation of $d\mu\text{DMD}$ from DFT:

DEFINITION D.16 (Relative distance to DFT).

$$(D.15) \quad \text{Relative distance to DFT}[\theta, d] := \frac{\|\mathbf{c}^*[(\mathbf{Z}_{d\text{-delayed}})_{\text{ms}}] + \mathbf{1}_\theta\|}{\sqrt{\theta}}$$

Remark D.17. By construction, **Relative distance to DFT** is non-negative. Yet, it can only have a maximum value of 1. To see this, define $(\mathbf{X}_{d\text{-delayed}})_{\text{ms}}$ as the submatrix corresponding to the first θ columns of $(\mathbf{Z}_{d\text{-delayed}})_{\text{ms}}$:

$$(\mathbf{Z}_{d\text{-delayed}})_{\text{ms}} =: [(\mathbf{X}_{d\text{-delayed}})_{\text{ms}} \mid (\mathbf{Z}_{d\text{-delayed}})_{\text{ms}} \mathbf{e}_{\theta+1}].$$

²⁰Analogous to [Lemma D.1](#)

²¹As described in [Definition 4.8](#).

Now, the proof of [Theorem 4.1](#) tells us that,

$$\mathbf{c}^*[(\mathbf{Z}_{\text{d-delayed}})_{\text{ms}}] = \mathcal{P}_{\mathcal{R}((\mathbf{x}_{\text{d-delayed}})_{\text{ms}}^H)}(-\mathbf{1}_\theta).$$

Substituting this in [Definition D.16](#), and using the identity,

$$I = \mathcal{P}_{\mathcal{N}((\mathbf{x}_{\text{d-delayed}})_{\text{ms}})} + \mathcal{P}_{\mathcal{R}((\mathbf{x}_{\text{d-delayed}})_{\text{ms}}^H)},$$

we have:

$$\begin{aligned} \text{Relative distance to DFT}[\theta, d] &= \frac{\|\mathbf{c}^*[(\mathbf{Z}_{\text{d-delayed}})_{\text{ms}}] + \mathbf{1}_\theta\|}{\sqrt{\theta}} \\ &= \frac{\|\mathcal{P}_{\mathcal{R}((\mathbf{x}_{\text{d-delayed}})_{\text{ms}}^H)}(-\mathbf{1}_\theta) - (-\mathbf{1}_\theta)\|}{\sqrt{\theta}} \\ &= \frac{\|\mathcal{P}_{\mathcal{N}((\mathbf{x}_{\text{d-delayed}})_{\text{ms}})}(-\mathbf{1}_\theta)\|}{\|-\mathbf{1}_\theta\|} \\ &\leq 1. \end{aligned}$$

Hence, the term Relative distance to DFT is appropriate.